



5-1999

Electron-phonon effects in graphene and an armchair (10,10) single wall carbon nanotube

Lilia Milcheva Rapatinska Woods

Follow this and additional works at: https://trace.tennessee.edu/utk_graddiss

Recommended Citation

Woods, Lilia Milcheva Rapatinska, "Electron-phonon effects in graphene and an armchair (10,10) single wall carbon nanotube. " PhD diss., University of Tennessee, 1999.
https://trace.tennessee.edu/utk_graddiss/8948

This Dissertation is brought to you for free and open access by the Graduate School at TRACE: Tennessee Research and Creative Exchange. It has been accepted for inclusion in Doctoral Dissertations by an authorized administrator of TRACE: Tennessee Research and Creative Exchange. For more information, please contact trace@utk.edu.

To the Graduate Council:

I am submitting herewith a dissertation written by Lilia Milcheva Rapatinska Woods entitled "Electron-phonon effects in graphene and an armchair (10,10) single wall carbon nanotube." I have examined the final electronic copy of this dissertation for form and content and recommend that it be accepted in partial fulfillment of the requirements for the degree of Doctor of Philosophy, with a major in Physics.

Gerald D. Mahan, Major Professor

We have read this dissertation and recommend its acceptance:

Tom Callcott, Ted Barnes, John Quinn, Bob Compton

Accepted for the Council:

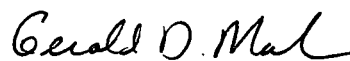
Carolyn R. Hodges

Vice Provost and Dean of the Graduate School

(Original signatures are on file with official student records.)


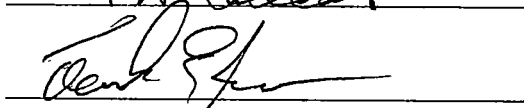


To the Graduate Council:

I am submitting herewith a dissertation written by Lilia Milcheva Rapatinska Woods entitled "Electron-Phonon Effects in Graphene and an Armchair (10,10) Single Wall Carbon Nanotube". I have examined the final copy of this document for form and content and recommend that it be accepted in partial fulfillment of the requirements for the Degree of Doctor of Philosophy, with a major in Physics.



Gerald D. Mahan, Major Professor

We have read this dissertation
and recommend its acceptance:

Accepted for the Council:



Associated Vice Chancellor
and Dean of the Graduate School

**ELECTRON-PHONON EFFECTS IN
GRAPHENE AND AN ARMCHAIR (10,10)
SINGLE WALL CARBON NANOTUBE**

A Dissertation

Presented for the

Doctor of Philosophy

Degree

The University of Tennessee, Knoxville

Lilia Milcheva Rapatinska Woods

May, 1999

ACKNOWLEDGEMENTS

I am very grateful to Dr. Gerald Mahan for serving as my thesis advisor; he has provided me with financial support, help and readiness to discuss seeking and solving interesting problems. It has been a pleasure to learn and work with somebody who has developed many new aspects of solid state physics.

I also wish to thank my other committee members - Dr. John Quinn, Dr. Ted Barnes, Dr. Tom Callcott and Dr. Bob Compton for the progress of my work.

I would like to thank my parents for their patience and their guidance during my life; my achievements wouldn't have been possible without their support. Finally, I wish to thank my husband, Gerald, for all his love, encouragement and understanding during my career as a PhD student. It is very admirable that he was completing his own PhD studies in physics at the same time.

ABSTRACT

New effects due to the electron-phonon interaction in some low-dimensional tight-binding systems are discussed. A sheet of graphite which is two dimensional and an armchair single wall carbon nanotube (SWNT) which is quasi-one dimensional are taken as examples. The geometrical structure and the linear dispersion of the energy with respect to the electron wave vector are expected to play a significant role. For the ordinary electron-phonon coupling which includes modulated hopping and linear electron-phonon interaction the matrix elements for both systems are derived in the context of a two parameter model for the phonon vibrational spectrum. It is found that they (for both structures) strongly depend on the geometry, display a deformation type of potential and are reduced by a factor of $(1 - R)$, where R depends uniquely on the introduced phonon parameters. Next a new type of interaction is derived; it arises from the phonon modulation of the electron-electron interaction. After writing the matrix elements for the new Hamiltonian, the problem is considered in the context of many body physics. There are two contributions. One of them is the random phase approximation with one phonon line. The electron self-energy for it is calculated. It is shown that, in general, one might expect that this is not a large effect. Analytical expressions are obtained for the armchair single wall carbon nanotube. The exchange interaction in the one-phonon approximation is another term that arises and is also considered. One is able to write four new Feynman diagrams and derive an expression for $-Im\Sigma(\vec{k})$. It is found that the contribution from this type of coupling could be large and comparable to the one from the modulated hopping. These results are supported by numerical estimates of some characteristics of graphene and SWNT. The values of the electron-phonon coupling constant, λ , and the electron lifetime, τ , could be compared between the traditional electron-phonon interaction and the phonon modulated electron-electron interaction. Finally, it is realized that for a

perfect (defect-free) armchair SWNT the diffusion thermopower and the phonon drag thermopower should be zero because of the complete symmetry of the energy bands of the system.

Contents

1	Overview	1
2	Lattice Dynamics in Graphene and a (10,10) SWNT	9
2.1	The model	9
2.2	Phonon spectrum for a (10,10) SWNT	14
2.3	Acoustic phonons for graphene and SWNT	16
3	Graphene	20
3.1	General considerations	20
3.2	Tight-binding band structure	21
3.3	Modulated hopping in terms of the tight-binding approximation	24
3.4	Deformation potential and optical phonon coupling	26
3.5	Electron-phonon and phonon-modulated electron-electron interactions	29
4	Synthesis, Structure and Applications of Single Wall Carbon Nanotubes	36
4.1	Synthesis of SWNT	36
4.2	Applications	39
4.3	Structure of an armchair and zigzag SWNT	40

5	Electron-Phonon Interactions In An Armchair SWNT	44
5.1	Tight-binding approach	44
5.2	Deformation potential approximation	48
5.3	Electron-phonon and phonon-modulated electron-electron interactions	50
6	Electron Self-Energy	54
6.1	Modulated hopping and linear electron-phonon interaction	54
6.2	RPA for the phonon modulated Coulomb interaction	58
6.2.1	Derivation of the Imaginary part of the electron self-energy	58
6.2.2	RPA for the armchair SWNT	62
6.3	Exchange self-energy	65
6.3.1	Derivation of the exchange self-energy	65
6.3.2	Application to SWNT	67
6.3.3	Application to graphene	68
7	Numerical Estimates of Some Transport Characteristics	70
7.1	Constant of interaction - λ	70
7.2	Thermoelectric power of a perfect armchair SWNT	74
8	Discussion	76
	Bibliography	82
	Appendices	87
A	Calculation of the Polarization Factor For the SWNT	88
B	Calculation of $S(k)$ for a tube	90
C	Calculation of $S(\vec{k})$ for Graphene	91

List of Figures

2.1	Phonon spectrum for graphene. The α and β dependence of the highly symmetrical points along all four branches are also given. .	10
2.2	Phonon spectrum for graphene with $\alpha = 8.98N/m^2$ and $\beta = 0.4N/m^2$	14
2.3	Brillouin zone for a SWNT.	15
2.4	Phonon Spectra of a (10,10) SWNT for a) $m=0$; and b) $m=1$. . .	17
3.1	Structure of graphene	21
3.2	Brillouin zone of two-dimensional graphite	22
4.1	Example of two types of SWNT from the many possible tubes . .	38
4.2	An example for a chiral vector is given - $\vec{C}_h = 3\vec{a}_1 + 2\vec{a}_2$. Point M can be mapped into point O by rolling the graphite sheet into a cylinder	41
4.3	The tube axis for the two highly symmetrical cases - zigzag and armchair - are shown.	42
4.4	a - Brillouin zone for an armchair tube; b - Brillouin zone for a zigzag tube	42
5.1	x-axis is the zigzag tube axis; y-axis is the armchair tube axis . .	46
5.2	Energy bands for an infinitely long (10,10) armchair carbon nanotube	47
6.1	Diagram for the first order electron-phonon interaction	55

6.2	Only the two lowest bands that cross the Fermi level at the Brillouin zone edge are of interest.	57
6.3	a - Feynman diagram with two Coulomb lines and one phonon line; b - RPA with one phonon line	59
6.4	Diagrams for the exchange interaction with one phonon line . . .	67
6.5	J as a function of x in 1D	68
6.6	J as a function of x in 2D	69

List of Tables

8.1	Numerical values for λ and τ for a tube	79
8.2	Numerical values for λ and τ for graphene	79

Chapter 1

Overview

The interaction between electrons and phonons is extremely important in the context of the flow of electricity and heat in a certain system. The discussion in this work will be primarily concerned with interesting transport properties in low-dimensional tight-binding systems. A long list of research - theoretical and experimental - has shown that properties in electronic materials that are reduced to one and two dimensions show fascinating new phenomena. A lot of scientists share the opinion that a big part of the future of technology belongs to the low-dimensional structures. They play a significant role not only in making new devices, but also in testing the laws of fundamental physics [1].

The aim of this work is geared towards a description of some new effects that arise when we consider the electron-phonon interaction in certain low dimensional tight-binding systems. These effects are demonstrated in a layer of graphite (called graphene) which is an example of a two-dimensional system, and an armchair single wall carbon nanotube (SWNT) which is an example of a quasi-one dimensional system (later we specify what an armchair (SWNT) is). The newly discovered carbon nanotubes offer the possibility to study the laws of solid state physics and search for new effects [2]. In fact, these nanoparticles served as an inspiration of

the present work.

A carbon nanotube is a graphite sheet rolled into a cylinder; its diameter is much smaller than its length. Because of the different ways this can be done, we expect that these quasi-one dimensional systems will display a very strong dependence on the geometry, but will also have similarities with the two dimensional graphene. This is unique to solid state physics. Every tube is characterized by a chiral index (n, m) which contains two integers and they specify the carbon nanotube uniquely (see Ch.4). In fact, their electronic structure is either metallic or semiconducting depending on how the sheet is rolled into a cylinder [3] (hence on the combination of n and m). Thus, it is very important to understand how the two-dimensional graphite will be described and then apply the formalism to the quasi-one dimensional SWNT.

Many of the applications of the carbon nanotubes are not realized yet, because this is a relatively new field of research. But, we can be certain that the properties and applications of the tubes will depend strongly on their geometry and low dimensionality. In principle we can imagine that a material with desired properties can be achieved using only carbon atoms and changing the geometrical structure.

To study the effects of any type of interaction one needs to understand first the electronic structure of the system. The electronic structure of two dimensional graphite - called graphene - is derived by a simple tight-binding scheme for the π -electrons of the carbon atoms [28]. The tight-binding approach is a good approximation here because the electrons are well localized around the ions. The structure of a single wall carbon nanotube can be obtained from that of graphene simply by using periodic boundary conditions in the circumferential direction - the wave vector associated with this dimension is quantized while the wave vector associated with translation is continuous. Therefore, the energy bands consist of a set of one dimensional dispersions.

All of the discussions and derivations will be concerned with one special case

of a highly symmetrical carbon nanotube - an armchair (10,10) SWNT, which is of metallic type. The reason is that the majority of the synthesized tubes and “ropes” are believed to be made of this kind of SWNT. The key to the production of the nanotubes is the use of metal catalyst such as Ni, Co or Fe [17] in an arc discharge method, or using a pulsed laser vaporization techniques [18]. The experimental analysis shows that most of the nanotubes are (10,10) SWNT.

The primary objective of this work will be to determine the electron-phonon interaction both the application of the known mechanisms and search for new ones. But, before we are able to do that the phonon dispersion relationships need to be derived. The phonon spectra for graphene [5], [6] and different SWNT-s [16] are known, and have been calculated up to fourth neighbors. The phonon dispersions need to be incorporated in the considerations of the electron-phonon effects. One needs to have a relatively simple relation of $\omega(\vec{Q})$ in order to do that properly. For this purpose a model with two parameters is proposed - the parameters are for the central force (α) and for the angle bending (β) that involves a three-body force. It turns out that all the features of the known graphene spectrum can be reproduced by a suitable choice of these two parameters. The same choice for α and β is used for the armchair tube. In most ionic and semiconducting solids only acoustic modes are important (if the band is nondegenerate). But for graphene and SWNT the optical modes depend on the acoustic ones. Thus, the optical modes cannot be simply neglected. This coupling was not considered in prior work and we therefore believe that the electron-phonon interaction needs to be calculated properly for both systems.

We start with the description of the electron-phonon interaction - an electron which is conceived to be in a particular state is described by a tight-binding wave function and a phonon is described by a phonon eigenstate. The finite resistivity of metals is entirely due to deviations of the ions from their equilibrium positions. The most important such deviations are those associated with the

thermal vibrations of the atoms. This is an intrinsic source of resistivity even for materials free of defects. The simplest theories of the lattice contribution to the conductivity of metals assume that the scattering is dominated by processes in which an electron emits (or absorbs) a single phonon; the energy of the electron changes by the energy of the phonon. It is a well known result that the electrical resistivity is proportional to the temperature T in the limit of high temperatures because the total number of phonons is directly proportional to T . In describing the electron-phonon interaction of a sheet of graphite and an armchair SWNT we will be concerned with the high temperature limit [8].

The simplest interpretation is that the vibrating ions carry the electron orbitals with them as they move - this is the so-called rigid ion approximation. This is certainly a great simplification because an important effect is neglected - the electron distribution will distort around the moving ion. But in tight-binding systems where the electrons are well localized the rigid ion approximation is a very reasonable approach. The quantitative description starts with the assumption that the periodic potential of a set of rigid ions $U_{per} = \sum_{\vec{R}} V(\vec{r} - \vec{R})$ is only an approximation of the true nonperiodic potential

$$U(\vec{r}) = U_{per}(\vec{r}) - \sum_{\vec{R}} \vec{u}(\vec{R}) \cdot \nabla V(\vec{r} - \vec{R}). \quad (1.1)$$

The potential $V(\vec{r} - \vec{R})$ is defined as the unscreened electron-ion potential. In the following discussions we will not be concerned with including screening effects.

In graphene the excited electron states are at the energy band minimum [29], which is the K point of the Brillouin zone. The K -point is located at the Brillouin zone edge. In this case only electrons with long wavelengths are involved. Thus, instead of calculating the potential one parametrizes it by assuming that it is proportional to the relative distance between nearest neighbors only. We will assume that this is true for the carbon nanotube also.

With the above substitution for the potential in these tight binding systems the

electron-phonon interaction comes into play through the hopping of the conduction electrons between nearest neighbors only. The lattice vibrations will modulate the process and the coupling is called modulated hopping. This kind of transition displays a deformation type. We obtain that by taking only phonons with long wavelength and polarizations of the ions $\hat{\eta} \rightarrow \hat{Q}$.

It is very important to calculate the matrix elements for this process correctly in order to have correct estimation of properties which depend on the matrix elements. The interaction Hamiltonian is written for a solid with two atoms per unit cell. Retaining only nearest neighbor hopping we are able to obtain that the matrix elements are linear in the phonon wave vector \vec{Q} and depend on both the acoustic and optical phonon modes. Therefore, one needs to have an appropriate model to account for the phonon polarizations. This was the reason for introducing the two parameter model for the phonon dynamics. Since the optical modes depend on the acoustic ones it turns out that the deformation constant D of the interaction is significantly reduced by a factor which depends only on the α and β parameters from the phonon model. This was not obtained in previous calculations [34], [40]. Another feature of note is that D is the same for graphene and for a tube; the nearest neighbor overlap integral is assumed the same and the curvature of the tube is not considered.

Another source of the electron-phonon interaction is when the potential is taken to be $\frac{Ze^2}{|\vec{r}-\vec{R}|}$. The formalism allows for introducing the charge distribution of the electrons and the ions of the crystal - $\rho_i(\vec{r})$ and $\rho_e(\vec{r})$. Since the electrons in graphite are π -electrons the electron, charge distribution is taken to have $2p_z$ -wave symmetry and the distribution for the ions has $2s$ -wave symmetry. $\rho_i(\vec{r})$ and $\rho_e(\vec{r})$ modulate the potential in such a way that in the long wavelength limit - $\vec{Q} \rightarrow 0$ the interaction takes the form of a deformation type again. It is possible to obtain the deformation constant \tilde{D} which depends on the parameters that describe the electron and ion charge distributions.

The last contribution that is discussed is new. It is the phonon modulated electron-electron interaction. It could be important not only for graphene but also for other low dimensional tight binding systems [4]. The potential is again the Coulomb potential between an electron and an ion (the same one as for the previous interaction). One notices that the position of the atom which is included in the potential is modulated by the lattice vibrations. Keeping only terms of first order in the ion displacements around equilibrium, one is able to obtain the form of the Hamiltonian. It is notable that this is not a phonon mediated electron-electron interaction [33] in which the coupling of the electrons is done by emitting or absorbing of a phonon. The phonon modulated electron-electron interaction has a different origin; it comes from the modulated distance of the charged ions. The matrix elements we derive are the same for transitions in graphene and a carbon nanotube, to a relative phase factor.

The next thing that is interesting to discuss is some aspects of the interacting electron-phonon system which are of many-body character - a charge carrier is linearly coupled to a systems of boson particles (phonons). The imaginary part of the electron self-energy is a very important quantity. It is closely related to the coupling constant of the interaction - λ and the electron lifetime - τ . We work in the one phonon approximation at finite temperatures. The Feynman diagram for the modulated hopping and the linear electron-phonon interaction is the same and it is well known. The only thing that needs to be done is to have the correct expressions of the coupling constant which is the same for both type of processes but with different deformation constants.

The new type of interaction that was introduced is expected to have strong impact on the many body effects also. There are two contributions to the electron self-energy. One of them comes from the diagrams that represent the random phase approximation of the system with one phonon line. Using the Lehmann representation one is able to derive a general expression for the self-energy that

resembles the one from the ordinary electron-phonon interaction. The general idea is that for small excitation energies this contribution can be neglected. In one dimension one needs to be more careful. It is already shown that the density oscillations and the spin waves completely describe the excitation spectrum in 1D [19]. For the quasi-one dimensional carbon nanotube with linear energy dispersions exact expressions can be found. A self-energy term that is proportional to T^2 and two terms proportional to T are produced. The coupling constant that corresponds to the T^2 term is a remnant of the plain electron-electron interaction. The terms with linear T can be considered to be a phonon modulation of the correlation energy.

Another contribution to the phonon modulation of the electron-electron interaction are the exchange terms. They arise from the different ways of pairing of the electron operators. There are four new diagrams that correspond to the new matrix elements. Again the diagrams involve only one phonon line. It is worth noting that the self-energy in this case depends only on the wave vector and not on the energy which means that the k_F will be left unchanged and it has little effect on the wave vector distribution. The interesting thing is that in the limit of $\vec{Q} \rightarrow 0$ the matrix elements can be written in the form of a deformation type of potential again. For both systems, graphene and a SWNT, the exchange terms are expected to give a large contribution.

To support the theoretical derivations with numbers, estimates of the coupling constant and the relaxation time for the different mechanisms of interaction are presented. The numbers support the expectations that the exchange phonon modulated electron-electron interaction will give a comparable contribution as the one from the modulated hopping.

Finally, we note that all of the discussion was done for graphene and an arm-chair single wall carbon nanotube without any defects or imperfections. If one introduces defects into the systems that will change the problem significantly, but

this is not a subject of the present work.

Chapter 2

Lattice Dynamics in Graphene and a (10,10) SWNT

2.1 The model

Here we present a model for the phonon spectrum of a two-dimensional sheet of graphite (called graphene). This is a natural starting point in obtaining the phonon spectrum for a SWNT. Since the structure and the bond lengths for an armchair (10,10) tube and graphene are very similar, one expects to obtain a very good approximation for the phonon modes of SWNT from the graphene spectrum. The measured and calculated spectrum for 2D graphite is presented in Fig.2.1. The method which is used in calculating the spectrum is the Born-von Karman lattice dynamical model and interactions up to fourth-neighbors are included [20]. The purpose of this work is not to improve on this approach, but to give a simpler alternative in obtaining the phonon dispersions. The vibrational modes for different carbon nanotubes are calculated in several reports [21], [24]. Results are also available for calculated and measured Raman- and Infrared-active modes [22], [23]. For considering the electron-phonon effects in the transport

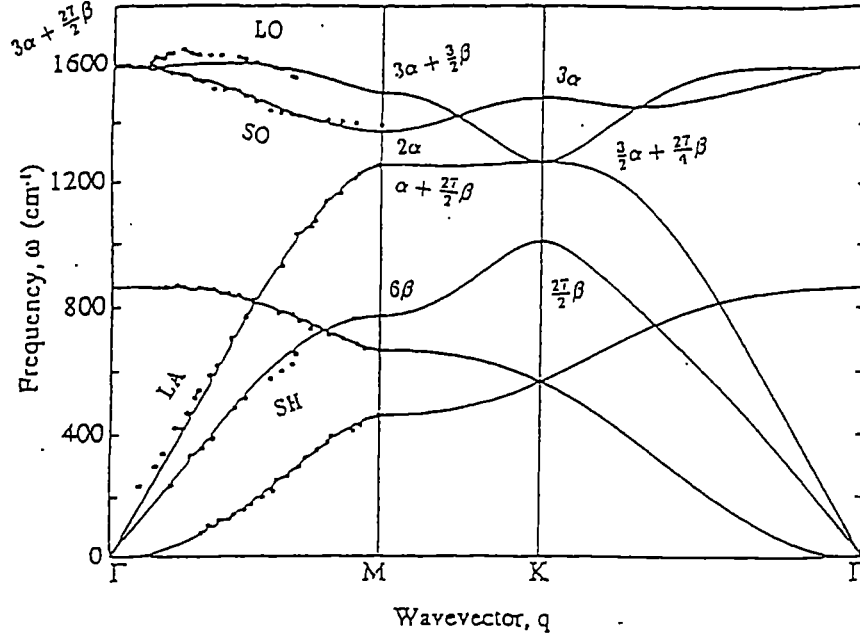


Figure 2.1: Phonon spectrum for graphene. The α and β dependence of the highly symmetrical points along all four branches are also given.

properties of an armchair SWNT one needs to incorporate the different modes and their polarizations in the expressions for the transport properties. It is not easy to do that with the Born-von Karman method. Here a model based on only two parameters is proposed, which enables one to obtain not only the phonon dispersions, but the polarization vectors as well. The two parameters are fitted to the well known spectrum for a layer of graphite. Notice that the proposed model describes only four of the branches of the phonon spectrum. They are denoted as LA, SH, LO and SO which correspond to in-plane vibrations only. The notation is taken from [5].

We assume that there are two types of forces between the atoms. One of them is a central force which depends only on the distance between two neighboring atoms. The potential which describes this force is given by

$$V = \frac{\alpha}{2} \sum_{nn'} [(\bar{u}_n - \bar{u}_{n'}) \cdot \hat{r}_{nn'}]^2, \quad (2.1)$$

where $\vec{u}_{n,n'}$ are the displacements of the atoms from their equilibrium positions, $\hat{r}_{n,n'}$ is the unit vector between those two atoms, and α is a constant which characterizes the central force.

The second type force is due to the bond-bending between the atoms. The potential is a three-body potential and was proposed in ref. [25] for obtaining the phonon spectrum for silicon. The model is described by

$$V = \frac{\beta}{2} \sum_{ijk} (\cos \theta_{ijk} - \cos \theta_0)^2, \quad (2.2)$$

where θ_{ijk} is the angle-formed between the $i - j$ bond and the $i - k$ bond. Thus, this potential is a three-body potential, because three neighboring atoms are involved. θ_0 is the equilibrium angle and for the hexagonal lattice is 120° . β is a characteristic constant for this type of force.

Thus, two parameters are introduced with this model. They will be determined from the known phonon spectrum for graphene.

From the graphite structure, the angle between two closest bonds is obtained to be

$$\cos \theta_{ijk} = \frac{[\vec{r}_{ij} + (\vec{u}_i - \vec{u}_j)] \cdot [\vec{r}_{ik} + (\vec{u}_i - \vec{u}_k)]}{|\vec{r}_{ij} + (\vec{u}_i - \vec{u}_j)| |\vec{r}_{ik} + (\vec{u}_i - \vec{u}_k)|}. \quad (2.3)$$

Since one is considering small displacements from equilibrium, the above expression can be expanded for small $\vec{u}_{i,j,k}$. After one does that, the result takes the form

$$\cos \theta_{ijk} = \left[-\frac{1}{2} - \left(\frac{\hat{r}_{ij}}{2} + \hat{r}_{ik}\right) \cdot (\vec{u}_i - \vec{u}_j) - \left(\frac{\hat{r}_{ik}}{2} + \hat{r}_{ij}\right) \cdot (\vec{u}_i - \vec{u}_k)\right]. \quad (2.4)$$

The constant $-\frac{1}{2}$ is canceled by $\cos \theta_0 = \cos 120^\circ = -\frac{1}{2}$. The microscopic equations for the normal modes are in the form

$$M\vec{u}_{ns} = \sum_{n's'} \vec{F}_{nsn's'} = -M\omega^2\vec{u}_{ns}. \quad (2.5)$$

Here $\vec{F}_{nsn's'}$ is the combined force due to the two potentials from eqn.(2.1) and eqn.(2.2). A nontrivial solution of these four equations exists if $|M(\vec{Q}) - M\omega^2(\vec{Q})I| =$

0, where $M(\vec{Q})$ is the dynamical matrix which is Hermitian and I is the unit matrix.

Thus, the matrix which needs to be diagonalized in order to obtain the normal modes is of the form

$$\begin{bmatrix} u - X_1 & F & A & C \\ F^* & u - X_2 & C & B \\ A^* & C^* & u - X_1 & F^* \\ C^* & B^* & F & u - X_2 \end{bmatrix} \quad (2.6)$$

with elements

$$\begin{aligned} u &= M\omega^2, \\ X_1 &= \frac{3\alpha}{2} + \frac{45\beta}{8} + \frac{9\beta}{8} \cos Q_y a, \\ X_2 &= \frac{3\alpha}{2} + \frac{45\beta}{8} - \frac{3\beta}{8} \cos Q_y a + \frac{3\beta}{2} \cos \frac{Q_x a \sqrt{3}}{2} \cos \frac{Q_y a}{2}, \\ F &= \frac{3\sqrt{3}\beta}{8} i (\sin Q_y a - 2e^{-i\frac{Q_x a \sqrt{3}}{2}} \sin \frac{Q_y a}{2}), \\ A &= e^{-i\frac{Q_x a}{2\sqrt{3}}} (\alpha e^{i\frac{Q_x a \sqrt{3}}{2}} + (\frac{\alpha}{2} + \frac{27\beta}{4}) \cos \frac{Q_y a}{2}), \\ C &= -(\frac{\alpha\sqrt{3}}{2} - \frac{9\sqrt{3}\beta}{4}) i e^{-i\frac{Q_x a}{2\sqrt{3}}} \sin \frac{Q_y a}{2}, \\ B &= e^{-\frac{Q_x a}{2\sqrt{3}}} (\frac{9\beta}{2} e^{i\frac{Q_x a \sqrt{3}}{2}} + (\frac{3\alpha}{2} + \frac{9\beta}{4}) \cos \frac{Q_y a}{2}), \end{aligned}$$

where $a = \sqrt{3}a_{C-C}$. The distance between two carbon atoms is $a_{C-C} = 1.42 \text{ \AA}$.

The goal is to solve for the normal modes for different symmetry points in the Brillouin zone of graphite since the fourth-order equation which arises from the above matrix cannot be solved analytically in general. After one obtains simplified expressions for the modes at different symmetry points, one compares with the known phonon spectrum for graphite (Fig.(2.1)) in order to find the best numbers for the model parameters α and β .

Simple results can be found if we look at the Γ , K and M points in the Brillouin

zone;

$$M\omega_{\Gamma,1,2}^2 = 0, \quad (2.7)$$

$$M\omega_{\Gamma,3,4}^2 = 3\alpha + \frac{27\beta}{2}, \quad (2.8)$$

$$M\omega_{K,1} = 3\alpha, \quad (2.9)$$

$$M\omega_{K,2} = \frac{27\beta}{2}, \quad (2.10)$$

$$M\omega_{K,3,4} = \frac{3\alpha}{2} + \frac{27\beta}{8}, \quad (2.11)$$

$$M\omega_{M,1}^2 = 3\alpha + \frac{3\beta}{2}, \quad (2.12)$$

$$M\omega_{M,2}^2 = 2\alpha, \quad (2.13)$$

$$M\omega_{M,3}^2 = \alpha + \frac{27\beta}{2}, \quad (2.14)$$

$$M\omega_{M,4}^2 = 6\beta. \quad (2.15)$$

Obviously, there are more constraints here than parameters. But, nevertheless, all the characteristic features of the phonon spectrum for graphene are obtained. At the Γ -point the two lower modes start at zero frequency and the higher modes start from the same nonzero value. At the K -point two of the modes are degenerate - the longitudinal optical and the longitudinal acoustic modes have a common frequency (Fig.2.1).

To find the best fit for the parameters α and β one has to look at the problem of interest. Here we are interested in the longitudinal acoustic branch. A good approximation of the LA branch can be obtained by choosing $\alpha = 8.98 \text{ N/m}^2$ and $\beta = 0.4 \text{ N/m}^2$. The graphene spectrum for these values is presented in Fig.2.2. It is seen from the graph that the lower branches are described fairly well while the upper branches are shifted upward although they retain the general features of the graphene spectrum as is shown in Fig.2.1

To describe the longitudinal optical phonons one can take for $\alpha = 7.27 \text{ N/m}^2$ and $\beta = 0.05 \text{ N/m}^2$. It is interesting to see that one of the other two branches,

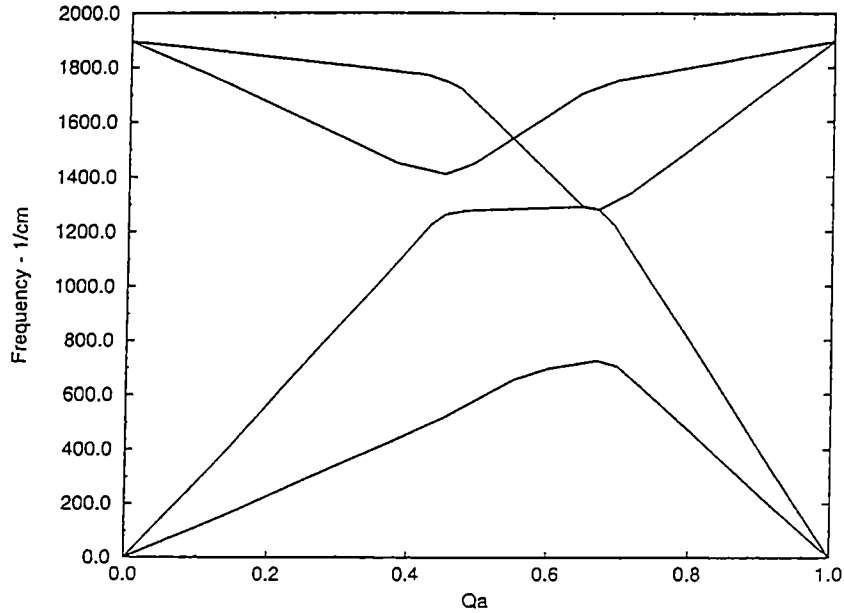


Figure 2.2: Phonon spectrum for graphene with $\alpha = 8.98 N/m^2$ and $\beta = 0.4 N/m^2$

which is a mixture between longitudinal and transverse modes, is characterised by the β parameter only - a good fit is $\beta = 0.83 N/m^2$. The other one depends only on α - choose for example $\alpha = 8.0 N/m^2$.

Therefore, depending on which part of the phonon spectrum one is interested in one can choose the appropriate values for the constants α and β .

2.2 Phonon spectrum for a (10,10) SWNT

The motion of the lattice is discussed by introducing two parameters for the central force potential and for the bond-bending potential. It is believed that this model would give good results when applied to the calculation of real transport properties such as electron lifetime and electrical conductivity.

To obtain the phonon dispersion relations and the polarization vectors for a SWNT we explore the connection between the structure of the tube and the carbon sheet and also we take into account that the tube is essentially a one-dimensional

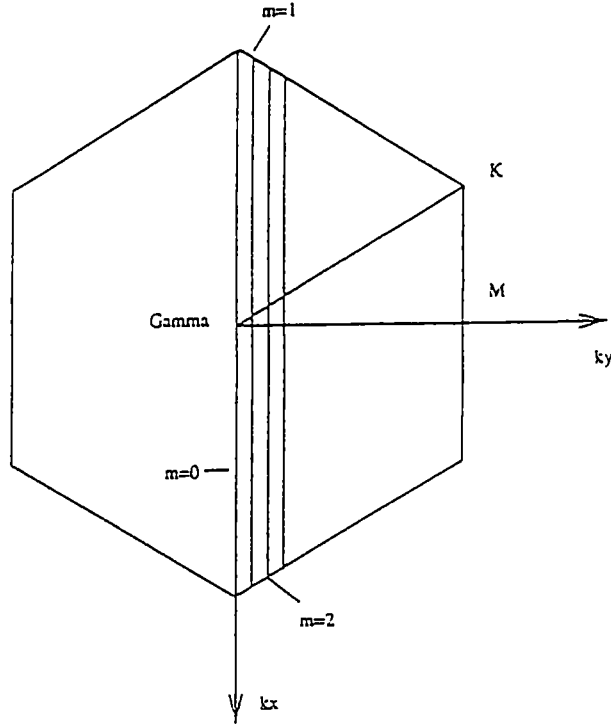


Figure 2.3: Brillouin zone for a SWNT.

system. The translational symmetry of the armchair SWNT persists along the tube axis, but does not longer exist around the circumference. The phonon wave vector is discrete in this direction and just like in the case for electrons takes discrete values

$$Q_x = \frac{m}{N} \frac{2\pi}{\sqrt{3}a}, \quad (2.16)$$

where $N = 10$ and $m = 0, \dots, N - 1$. Thus, the 4×4 matrix for graphene can be turned into a matrix for the (10,10) tube by substitution the above condition in eqn.(2.5) and by keeping $Q_y = Q$ continuous (for more details - see Chapters (3) and (4)).

The discrete set of allowed values for Q_x implies that the Brillouin zone for graphene will be sliced N times - Fig.2.3. Thus, one obtains a set of phonon branches for each m . The calculated spectra for different types of tubes using this zone-folding technique can be found in [26].

For this problem we are interested in transport properties where the acoustic modes are important. This means that only the modes and the polarization

vectors around the Γ -point need to be determined. Results for $m = 0$ and $m = 1$ are given on Fig.2.4. α and β have the same values as for graphene.

We see that the general properties for the acoustic and optical modes are preserved with this method. For longitudinal acoustic modes the ions oscillate in phase along the tube axis and for the longitudinal optical modes they are out of phase. The phonon frequency for the longitudinal branch changes linearly with respect to k while the optical ω stays a constant. One is able to determine the velocity of sound, s , also. For $m = 0$ we obtain that $s_{1D} = 3.26 * 10^5 \text{ cm/s}$ while for graphene $s_{2D} = 7.5 * 10^5 \text{ cm/s}$.

2.3 Acoustic phonons for graphene and SWNT

Here we discuss the equations for the phonons in graphene and the (10,10) SWNT. It is evident from the form of the matrix elements for the electron-phonon interaction that the quantity $(\hat{\eta}_A - \hat{\eta}_B)$ need to be determined. The terms from the dynamical matrix are determined for small wave vectors;

$$X_1 = \frac{3\alpha}{2} + \frac{27\beta}{4} - \frac{9}{16}\beta Q_y^2 a^2, \quad (2.17)$$

$$X_2 = \frac{3\alpha}{2} + \frac{27\beta}{4} - \frac{9}{16}\beta Q_x^2 a^2, \quad (2.18)$$

$$F = -\frac{9}{16}\beta Q_x Q_y a^2, \quad (2.19)$$

$$A = \frac{3\alpha}{2} + \frac{27\beta}{4} + iQ_x a \frac{\sqrt{3}}{2} \left(\frac{\alpha}{2} - \frac{9}{4}\beta \right), \quad (2.20)$$

$$C = -iQ_y a \frac{\sqrt{3}}{2} \left(\frac{\alpha}{2} - \frac{9}{4}\beta \right), \quad (2.21)$$

$$B = \frac{3\alpha}{2} + \frac{27\beta}{4} - iQ_x a \frac{\sqrt{3}}{2} \left(\frac{\alpha}{2} - \frac{9}{4}\beta \right). \quad (2.22)$$

Now by adding and subtracting the microscopic equations, they can be written in such a way that a solution for $(A_{x,y} - B_{x,y})$ in terms of $(A_{x,y} + B_{x,y})$ is found.

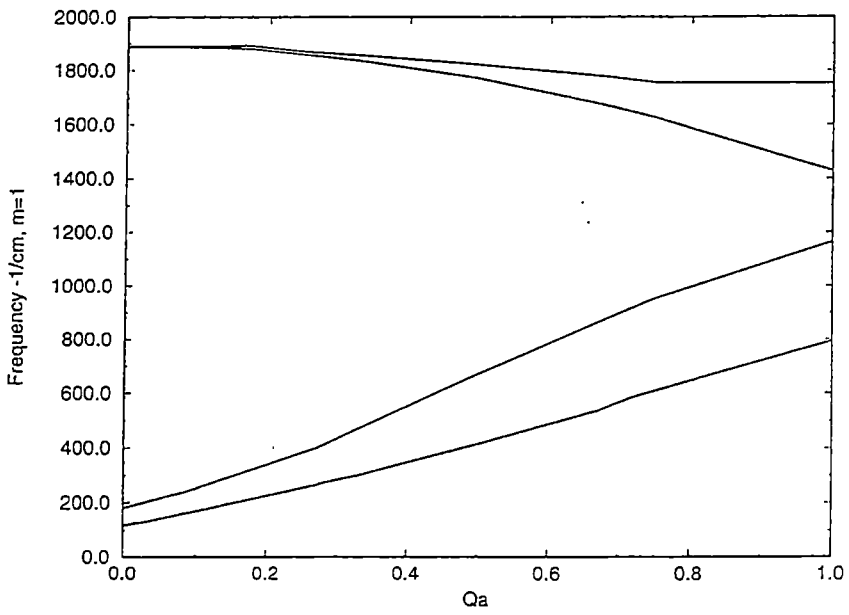
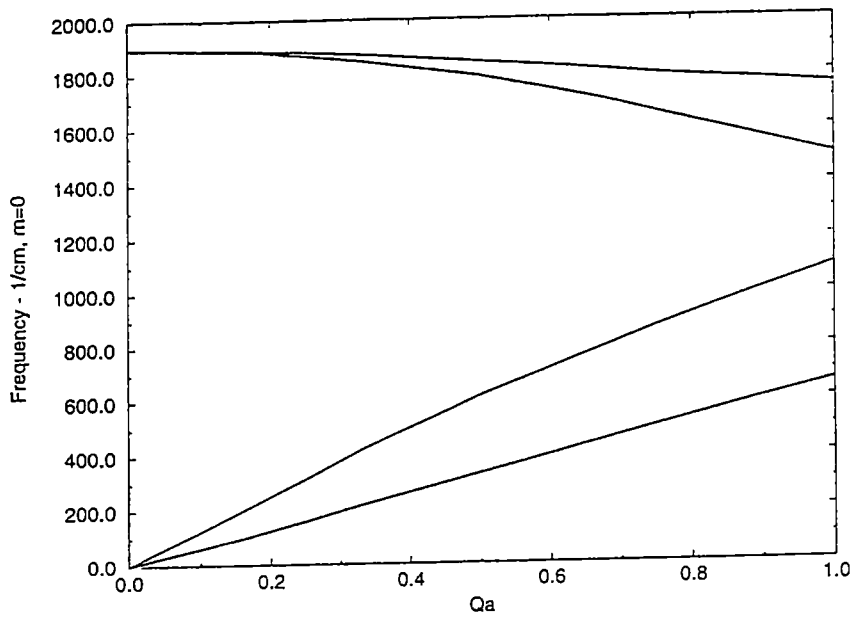


Figure 2.4: Phonon Spectra of a (10,10) SWNT for a) $m=0$; and b) $m=1$

By $A_{x,y}$ and $B_{x,y}$ we denote the polarization vectors $\hat{\eta}_A$ and $\hat{\eta}_B$.

$$\begin{aligned} M\omega^2(A_x + B_x) &= -Q_y^2 a^2 D_r(A_x + B_x) + iQ_y a D_i(A_x - B_x) \\ &+ Q_x Q_y a^2 D_r(A_y + B_y) - iQ_y a D_i(A_y - B_y), \end{aligned} \quad (2.23)$$

$$\begin{aligned} M\omega^2(A_x - B_x) &= -iQ_x a D_i(A_x + B_x) + (G - Q_y^2 a^2 D_r)(A_x - B_x) \\ &+ iQ_y a D_i(A_y + B_y) + Q_x Q_y a^2 D_r(A_y - B_y), \end{aligned} \quad (2.24)$$

$$\begin{aligned} M\omega^2(A_y + B_y) &= Q_x Q_y a^2 D_r(A_x + B_x) - iQ_y a D_i(A_x - B_x) \\ &- Q_x^2 a^2 D_r(A_y + B_y) - iQ_x a D_i(A_y - B_y), \end{aligned} \quad (2.25)$$

$$\begin{aligned} M\omega^2(A_y - B_y) &= iQ_y a D_i(A_x + B_x) + Q_x Q_y a^2 D_r(A_x - B_x) \\ &- iQ_x a D_i(A_y + B_y) + (G - Q_x^2 a^2 D_r)(A_y - B_y). \end{aligned} \quad (2.26)$$

The following definitions are made;

$$\begin{aligned} D_r &= \frac{9}{16}\beta, \\ D_i &= \frac{\sqrt{3}}{4}\left(\alpha - \frac{9}{2}\beta\right), \\ G &= 3\alpha + \frac{27}{2}\beta. \end{aligned}$$

The acoustic modes are the ones in eqns.(2.23,2.25) and the optical modes are those in eqns.(2.24,2.26). We see that they are coupled; although the acoustic modes are of interest for us, we have to account for the optical modes also. This is so, because in the matrix elements for the electron-phonon coupling both polarizations enter the formulas.

Now only the terms with first order wave vector are kept in the expressions for the optical modes. Thus, we are able to write

$$(A_x - B_x) \approx i \frac{\sqrt{3}}{12} \frac{(\alpha - \frac{9}{2}\beta)}{(\alpha + \frac{9}{2}\beta)} [Q_x a(A_x + B_x) - Q_y a(A_y + B_y)], \quad (2.27)$$

$$(A_y - B_y) \approx -i \frac{\sqrt{3}}{12} \frac{(\alpha - \frac{9}{2}\beta)}{(\alpha + \frac{9}{2}\beta)} [Q_x a(A_y + B_y) + Q_y a(A_x + B_x)]. \quad (2.28)$$

If one uses our fitted values for the force constants one can estimate that the factor $R = \frac{\alpha-9/2\beta}{\alpha+9/2\beta} \approx 0.67$.

The above derivations are for a two-dimensional layer of graphite. From here it is easy to derive the optical modes for a SWNT. Set $Q_x = 0$ and keep $Q_y = Q$ continuous. Then the expressions become

$$(A_x - B_x) = -i\frac{\sqrt{3}}{12}RQa(A_y + B_y), \quad (2.29)$$

$$(A_y - B_y) = -i\frac{\sqrt{3}}{12}RQa(A_x + B_x). \quad (2.30)$$

Therefore, the conclusion is that in further calculations the optical modes cannot be neglected because they couple to the acoustic ones according to the above results.

Chapter 3

Graphene

3.1 General considerations

Here we discuss a single plane of graphite which is called graphene. The carbon atoms are arranged as in Fig.3.1. As it was said earlier the nearest neighbors are separated by $a_0 = 1.42 \text{ \AA}$. Carbon has four valence electrons. Three of them are tightly σ -bonded with neighboring atoms in the layer. The remaining electron goes into a p -state oriented perpendicular to the plane and is analogous to the π state of a diatomic molecule. The three electrons involved in co-planar bonds will not play a significant role in the transport properties of the graphene. Therefore, the atom will be treated as having one conduction electron which is considered to be in the $2p_z$ state.

Because of the small overlap of the π -wave functions in graphite their levels split in the solid much less than the σ -bands. The bonding and antibonding π -bands overlap somewhat, so that the two atoms in the unit cell do not fill the bonding band completely. It turns out that there is no band gap between the empty and full states, but there are only very few states near the top of the occupied region. Because of this, graphite is called a semimetal.

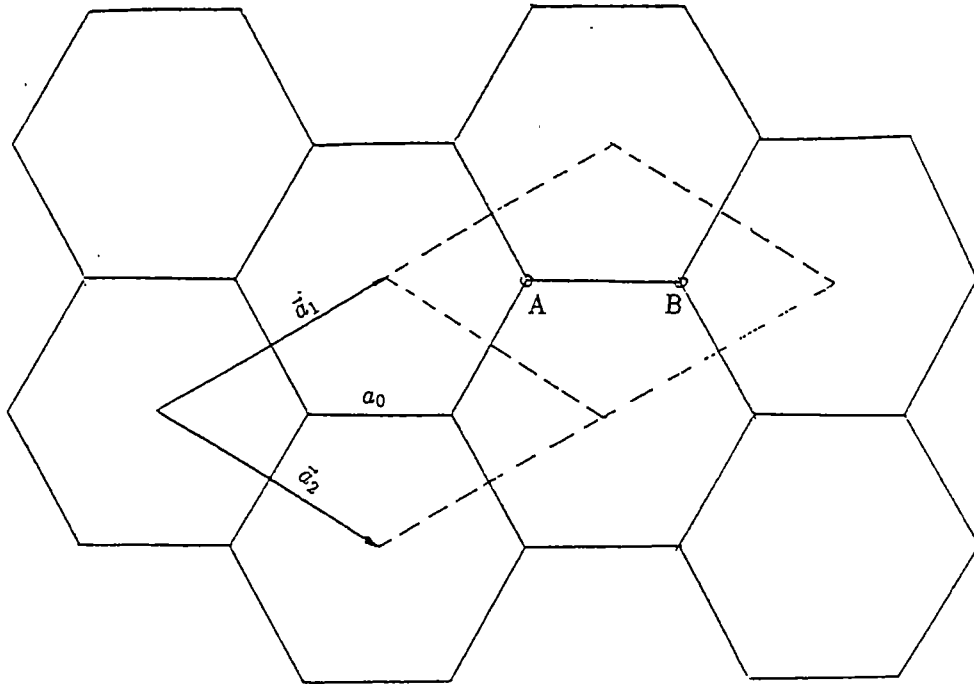


Figure 3.1: Structure of graphene

The unit cell for a graphite sheet is of hexagonal form with two atoms per unit cell which we call A and B atoms. The convention which we will follow is that any point in the sheet of hexagons can be mapped by the two fundamental lattice displacement vectors \vec{a}_1 and \vec{a}_2 as shown in Fig.3.1. The magnitude of the vectors is $a = a_0 \times \sqrt{3} = 2.46 \text{ \AA}$. Thus, the first Brillouin zone (BZ) is of hexagonal form - Fig.3.2. The sides of the hexagon are at a distance $\frac{1}{\sqrt{3}a}$ from the center. Γ , M and K are some of the high symmetry points which are also shown on Fig.3.2.

3.2 Tight-binding band structure

In developing the method we assume that around each lattice point the full periodic crystal Hamiltonian can be approximated by H_{at} of a single atom situated at this lattice point. We also assume that the electron levels of the atomic Hamiltonian are well localized, which is true for the carbon orbitals in graphene. This means that the tight-binding approximation (TBA) is a very reasonable approach

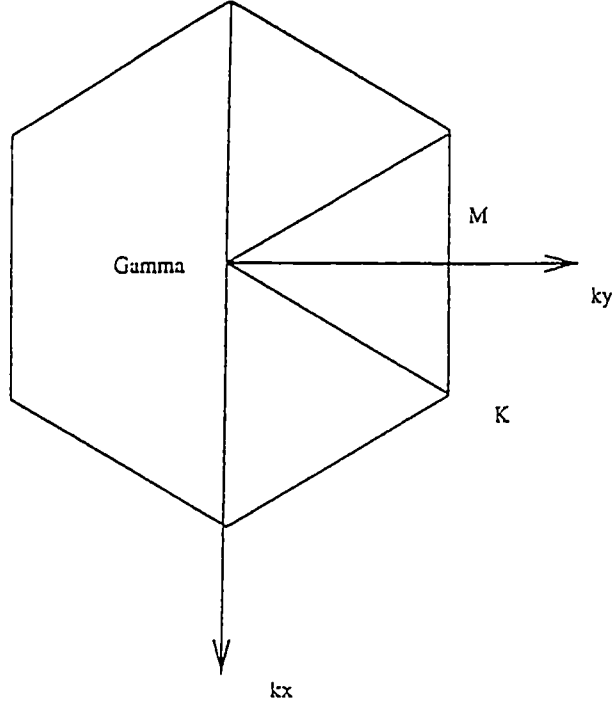


Figure 3.2: Brillouin zone of two-dimensional graphite

in our case [27].

The wave functions are chosen to satisfy the Bloch condition, but at the same time they reflect the atomic character of the levels. For graphene they are of the form

$$\psi = \sum_{nn'} [e^{i\vec{k}\cdot\vec{R}_n} f(\vec{r} - \vec{R}_n) + \lambda_{nn'} e^{i\vec{k}\cdot\vec{R}_{n'}} f(\vec{r} - \vec{R}_{n'})], \quad (3.1)$$

where $n, n' = A, B$ for the two different atoms in the unit cell. \vec{R}_n and $\vec{R}_{n'}$ are the positions of the atoms A and B . λ is a constant which will be determined later. The function $f(\vec{r})$ which is centered at A or B atoms describes the atomic nature of the electronic states - in this case it is a $2p_z$ orbital.

To proceed further with the problem we need to evaluate the constant λ in the wave functions and to obtain an energy dispersion relation. We do that by solving the equation

$$H\psi = E\psi \quad (3.2)$$

which could be written as

$$H_{nn} + \lambda_{nn'} H_{nn'} = ES, \quad (3.3)$$

$$H_{n'n} + \lambda_{nn'} H_{n'n'} = \lambda_{nn'} ES. \quad (3.4)$$

Here S is the normalization for the single electron orbital and

$$H_{nn'} = \int d^3r f(\vec{r} - \vec{R}_n)^* H f(\vec{r} - \vec{R}_{n'}). \quad (3.5)$$

Now keeping only nearest neighbor overlap integrals (the electron states are well localized) we obtain for the energy

$$E = \pm \frac{|H_{nn'}|}{S} \quad (3.6)$$

and for the constant

$$\lambda_{nn'} = \pm \frac{H_{nn'}^*}{|H_{nn'}|}. \quad (3.7)$$

Using the actual structure for graphene and keeping only nearest neighbors the expressions for the energy and the constant λ are found to be

$$E = \pm J_0 \frac{(1 + 4\cos\frac{\sqrt{3}k_x a}{2} \cos\frac{k_y a}{2} + 4\cos^2\frac{k_y a}{2})^{1/2}}{S}, \quad (3.8)$$

$$\lambda_{AB} = \pm \frac{e^{-ik_x \frac{a}{\sqrt{3}}} (1 + 2e^{ik_x \frac{a\sqrt{3}}{2}} \cos\frac{k_y a}{2})}{(1 + 4\cos\frac{\sqrt{3}k_x a}{2} \cos\frac{k_y a}{2} + 4\cos^2\frac{k_y a}{2})^{1/2}} \quad (3.9)$$

where $J_0 = 2.5 \text{ eV}$ [28] is the overlap integral between nearest neighbors. It is already shown [28], [29] that there are two symmetric bands that cross the Fermi surface at the K points in the BZ for graphene. It also could be derived that around the K -points for small wave vectors the energy dispersion relation is linear with respect to the electron wave vector.

3.3 Modulated hopping in terms of the tight-binding approximation

We are interested in electron-phonon coupling in graphene. In the tight-binding approximation one contribution to the electron-phonon interaction comes from the modulation of the tight-binding matrix elements arising from the change in the overlap between orbitals centered on different atoms and from the Coulomb potential (which is the case for normal metals). Thus, the tight-binding approach is the limit of total screening.

Further we derive a formula for the matrix elements for modulated hopping of the electron-phonon coupling. It is assumed that when the lattice is deformed by displacing an atom from its equilibrium position the orbitals follow the displaced atoms without appreciable deformation. Thus, the position of the ion is $\vec{R}_{A,B} = \vec{R}_{A,B}^0 + \vec{u}_{A,B}$ where the displacements $\vec{u}_{A,B}$ are small. Since the orthogonality relation of the well localized electronic states is still valid, we have

$$\{c_n^+, c_{n'}\} = \delta_{nn'}. \quad (3.10)$$

The Hamiltonian for the interaction for a crystal with two atoms per unit cell is given by [29]

$$H_{int} = \sum_{nn'} \int d^3r \psi^\dagger V(\vec{r} + \vec{R}_n^0 + \vec{u}_n - \vec{R}_{n'}^0 - \vec{u}_{n'}) \psi. \quad (3.11)$$

Now the potential for the rigid ions is expanded around the equilibrium positions as follows

$$V(\vec{r} + \vec{R}_n^0 + \vec{u}_n - \vec{R}_{n'}^0 - \vec{u}_{n'}) = V_0 + (\vec{u}_n - \vec{u}_{n'}) \cdot \nabla V(\vec{r} + \vec{R}_n^0 - \vec{R}_{n'}^0). \quad (3.12)$$

We substitute this into the expression for H_{int} and drop the constant term - V_0

$$H_{int} = \sum_{nn'} (\vec{u}_n - \vec{u}_{n'}) \cdot \int d^3r \psi^\dagger \nabla V(\vec{r} + \vec{R}_n^0 - \vec{R}_{n'}^0) \psi = \sum_{nn'} (\vec{u}_n - \vec{u}_{n'}) \cdot J_{nn'}, \quad (3.13)$$

where $J_{nn'}$ is the overlap integral. Note that the potential of the electron-phonon interaction is represented by a sum of atomic potentials centered around each ion.

The next step is to expand the displacements \vec{u}_n in terms of the phonon creation and annihilation operators b_Q and b_{-Q}^+ [30]

$$\vec{u}_n = \sum_{\vec{Q}} \sqrt{\frac{\hbar}{2NM\omega_Q}} \hat{\eta}_n e^{i\vec{Q}\cdot\vec{R}_n^0} (b_Q + b_{-Q}^+). \quad (3.14)$$

ω_Q is the frequency of the phonons and $\hat{\eta}_n$ is the polarization vector of the ion.

The electron field operators could be written in terms of the creation and annihilation operators for the electrons

$$\psi = \sum_{\vec{k}} \psi_\lambda(\vec{k}) c_{\vec{k}}, \quad (3.15)$$

where $\psi(\vec{k})$ is the wave function from eqn.(3.1) and λ is the band index. For graphite the part of the overlap integral $J_{nn'}$ which concerns the \vec{r} integration usually can be taken to depend only on the distance between two neighboring atoms [34]

$$J_{nn'} \sim \frac{(\vec{R}_n^0 - \vec{R}_{n'}^0)}{|\vec{R}_n^0 - \vec{R}_{n'}^0|} q_0 J_0, \quad (3.16)$$

where q_0 and J_0 are known constants. We use $q_0 = 2.2 \text{ \AA}^{-1}$, the number which is cited in ref. [34].

Now we take eqns. (3.14-3.16) and substitute them in the expression for the Hamiltonian - eqn.(3.13)

$$\begin{aligned} H_{int} &= \sum_{ij,nn'} \sum_{\vec{k}\vec{k}'\vec{Q}} q_0 J_0 \sqrt{\frac{\hbar}{2NM\omega_Q}} (\hat{\eta}_n e^{i\vec{k}\cdot\vec{R}_n^0} - \hat{\eta}_{n'} e^{i\vec{k}\cdot\vec{R}_{n'}^0}) \cdot \frac{(\vec{R}_n^0 - \vec{R}_{n'}^0)}{|\vec{R}_n^0 - \vec{R}_{n'}^0|} \\ &\times (\lambda_i^*(\vec{k}') e^{-i(\vec{k}'\cdot\vec{R}_{n'}^0 + \vec{k}\cdot\vec{R}_n^0)} + \lambda_j(\vec{k}) e^{-i(\vec{k}'\cdot\vec{R}_n^0 - \vec{k}\cdot\vec{R}_{n'}^0)}) \\ &\times c_{\vec{k}'}^+ c_{\vec{k}} (b_{\vec{Q}} + b_{-\vec{Q}}^+) \delta_{\vec{k}', \vec{k} + \vec{Q}}. \end{aligned} \quad (3.17)$$

This is a general formula for the modulated hopping electron-phonon interaction of a solid with two atoms per unit cell. For graphene all the vectors in the above

formulas are two dimensional. Now one can evaluate the matrix elements for the electron-phonon coupling. The constants λ are also present. They control the processes between different energy bands.

3.4 Deformation potential and optical phonon coupling

If we look at the Fermi surface [28] of the two-dimensional graphite we see that it has small circles around the K points in the Brillouin zone. Because of the symmetry of the system it is only necessary to consider one of them which we choose to be

$$\vec{k}_0 = \left(\frac{2\pi}{\sqrt{3}a}, \frac{2\pi}{3a} \right). \quad (3.18)$$

The electronic states of interest are in the vicinity of these points. The excited states are at the band minimum and they are located in a small wave vector space. One can also see that the K point is situated at the Brillouin zone edge. When we are concerned with transitions at the Brillouin zone edge the deformation potential approximation comes into play. The main idea is that only the long-wave limit $\vec{Q} \rightarrow 0$ in the first Brillouin zone is needed and only acoustic phonons are important. Also for the phonon energy we take $\omega_Q = sQ$ with s being the sound velocity in the layer. This is the deformation potential approximation. This approach was invented to describe simple metallic systems [31]. Now we can look how this method can be applied to graphene. Since we are interested what happens around the K -point we make an expansion around these points - $\vec{k} \rightarrow \vec{k}_0 + \vec{\tilde{k}}$ where $\vec{\tilde{k}}$ is a small vector. The energy has a linear dispersion

$$E = \pm v_F |\tilde{k}|, \quad (3.19)$$

where $v_F = J_0 \frac{\sqrt{3}a}{2}$ is the Fermi velocity. The expression for the constants λ becomes

$$\lambda_{AB} = \pm \frac{e^{-i\frac{2\pi}{3}}}{\tilde{k}} (\tilde{k}_y - i\tilde{k}_x) = \pm e^{-i(\frac{2\pi}{3} + \phi)}, \quad (3.20)$$

where the phase factor $\phi = \tan^{-1} \frac{\bar{k}_x}{\bar{k}_y}$ is introduced. The expression from eqn.(3.17) can be written in a more convenient form. For processes between different bands we have

$$\begin{aligned}
M_{\bar{k}\bar{k}',11} &= \sum_{AB} 2 \sqrt{\frac{\hbar}{2NM\omega_Q}} q_0 J_0 e^{i\frac{\phi'-\phi}{2}} \\
&\times \left[\hat{\eta}_A \cdot \hat{\nabla} R_{AB} \cos\left(\frac{2\pi}{3} - \bar{k}_0 \cdot \bar{R}_{AB} - \frac{\bar{Q} \cdot \bar{R}_{AB}}{2}\right) \right. \\
&+ \frac{\phi + \phi'}{2} e^{-i\frac{\bar{Q} \cdot \bar{R}_{AB}}{2}} \\
&+ \hat{\eta}_B \cdot \hat{\nabla} R_{BA} \cos\left(\frac{2\pi}{3} + \bar{k}_0 \cdot \bar{R}_{BA} + \frac{\bar{Q} \cdot \bar{R}_{BA}}{2}\right) \\
&+ \left. \frac{\phi + \phi'}{2} e^{-i\frac{\bar{Q} \cdot \bar{R}_{BA}}{2}} \right], \tag{3.21}
\end{aligned}$$

$$M_{\bar{k}\bar{k}',22} = -M_{\bar{k}\bar{k}',11}, \tag{3.22}$$

$$\begin{aligned}
M_{\bar{k}\bar{k}',12} &= \sum_{AB} 2 \sqrt{\frac{\hbar}{2NM\omega_Q}} q_0 J_0 e^{i\frac{\phi'-\phi}{2}} \\
&\times \left[\hat{\eta}_A \cdot \hat{\nabla} R_{AB} \sin\left(\frac{2\pi}{3} - \bar{k}_0 \cdot \bar{R}_{AB} - \frac{\bar{Q} \cdot \bar{R}_{AB}}{2}\right) \right. \\
&+ \frac{\phi + \phi'}{2} e^{-i\frac{\bar{Q} \cdot \bar{R}_{AB}}{2}} \\
&+ \hat{\eta}_B \cdot \hat{\nabla} R_{BA} \sin\left(\frac{2\pi}{3} + \bar{k}_0 \cdot \bar{R}_{BA} + \frac{\bar{Q} \cdot \bar{R}_{BA}}{2}\right) \\
&+ \left. \frac{\phi + \phi'}{2} e^{-i\frac{\bar{Q} \cdot \bar{R}_{BA}}{2}} \right], \tag{3.23}
\end{aligned}$$

$$M_{\bar{k}\bar{k}',21} = -M_{\bar{k}\bar{k}',12}, \tag{3.24}$$

where $\bar{R}_{AB} = \bar{R}_A^0 - \bar{R}_B^0$ and $\hat{\nabla} R_{AB} = \frac{(\bar{R}_A^0 - \bar{R}_B^0)}{|\bar{R}_A^0 - \bar{R}_B^0|}$. By M_{11} we mean the matrix element for transitions in the conduction band, M_{22} stands for transitions in the valence band and M_{12} and M_{21} are for transitions between the two. Further manipulations are possible with the above formulas, namely consider the limit for small \bar{Q} and expand around the K -point. Then one notices that two terms are present - one with $(\hat{\eta}_A + \hat{\eta}_B)$ which is responsible for the acoustic excitations and one with $(\hat{\eta}_A - \hat{\eta}_B)$ which is responsible for the optical excitations. Summing over

nearest neighbors and using the results from Ch.2 that both types of modes are coupled the final formulas for the matrix elements are obtained to be

$$\begin{aligned}
M_{11} = & -iq_0J_0X_Q \frac{\sqrt{3}}{4} [(\eta_{Ax} + \eta_{Bx})(Q_x a \cos \frac{\phi + \phi'}{2} + Q_y a \sin \frac{\phi + \phi'}{2}) \\
& + (\eta_{Ay} + \eta_{By})(Q_x a \sin \frac{\phi + \phi'}{2} - Q_y a \cos \frac{\phi + \phi'}{2})] (1 - R), \quad (3.25)
\end{aligned}$$

$$\begin{aligned}
M_{12} = & -iq_0J_0X_Q \frac{\sqrt{3}}{4} [(\eta_{Ax} + \eta_{Bx})(Q_x a \sin \frac{\phi + \phi'}{2} - Q_y a \cos \frac{\phi + \phi'}{2}) \\
& + (\eta_{Ay} + \eta_{By})(Q_x a \cos \frac{\phi + \phi'}{2} + Q_y a \sin \frac{\phi + \phi'}{2})] (1 - R). \quad (3.26)
\end{aligned}$$

Two conclusions can be made. First, the matrix elements for both transitions - intraband and interband - are reduced by a factor $(1 - R)$ which depends on the parameters chosen to describe the oscillations of the ions. Second, it is evident that not only the longitudinal modes are important, but also the transverse modes give a similar contribution. Both types of polarizations are present in M_{11} and M_{12} . Thus, there is a difference between this tight-binding system and a simple metal, in which only acoustic phonons are expected to matter. The formulas (3.25) and (3.26) disagree with the ones found in ref. [34] by a factor $(1 - R)$ which reduces the matrix elements. Also the dependance of $|M_Q|^2$ on the phonon wave vector Q is clearly displayed in the present calculation. Thus, we believe we have brought some enlightenment to the matter and in this way further calculations that rely on the matrix elements of the electron-phonon interaction can be done correctly.

The matrix elements can also be evaluated for the range of the optical phonons. In this case one assumes that the phonon energy ω_Q is constant. An optical phonon result when the neighboring atoms vibrate out of phase. This polarizes the system and is a cause for the presence of an electric field, which scatters the electrons. The coupling to optical phonons can be very large. To estimate it in this case one uses eqns.(3.21-3.24) with constant frequency and $(\hat{\eta}_A + \hat{\eta}_B)$ expressed in terms of $(\hat{\eta}_A - \hat{\eta}_B)$.

3.5 Electron-phonon and phonon-modulated electron-electron interactions

The model which we are discussing is a neutral tight-binding systems that has two atoms per unit cell. For graphite the ion cores have s -wave symmetry and the electrons that are responsible for the conduction process have p_z -wave symmetry. Since this is a neutral system the average number of conduction carriers on each side is equal to the valence of the ions. We also assume that the rigid ion approximation is valid and the electrons can hop to the neighboring sites. The starting Hamiltonian for such a system is written as

$$H = H_0 + H_{int}, \quad (3.27)$$

$$H_0 = -\gamma_0 \sum_{j\delta} (c_{j+\delta}^+ c_j + c_{j+\delta} c_j) + \sum_{\vec{Q}} \omega_{\vec{Q}} a_{\vec{Q}}^+ a_{\vec{Q}}, \quad (3.28)$$

$$H_{int} = \frac{e^2}{2} \sum_{nn'} \int \frac{d^3 r_1 d^3 r_2}{|\vec{r}_1 - \vec{r}_2|} [\rho_i(\vec{r}_1 - \vec{R}_n) - \rho_e(\vec{r}_1 - \vec{R}_n) c_n^+ c_n] \\ \times [\rho_i(\vec{r}_2 - \vec{R}_{n'}) - \rho_e(\vec{r}_2 - \vec{R}_{n'}) c_{n'}^+ c_{n'}], \quad (3.29)$$

where $\gamma_0 = J_0 = 2.5 \text{ eV}$ and ρ_i and ρ_e are the ion and electron charge densities. In the case of graphite where there are two atoms per unit cell the electron operators $c_{n,m}$ will be called A and B corresponding to the particular ions. Again $\vec{R}_{n,n'}$ are the locations of the positive ions. We want to express H_{int} in terms of collective coordinates. Thus, the first thing that needs to be done is to diagonalize H_0 . In TBA the electron operators are expanded in the form

$$c_n = \sum_{\vec{k}} e^{i\vec{k} \cdot \vec{R}_n^0} c_{\vec{k}}. \quad (3.30)$$

Therefore, the form for H_0 is just the usual hopping Hamiltonian which we already discussed in the previous sections.

$$H_0 = \gamma_0 \sum_{\vec{k}} [g(\vec{k}) A_{\vec{k}}^+ B_{\vec{k}} + g^*(\vec{k}) B_{\vec{k}}^+ A_{\vec{k}}], \quad (3.31)$$

$$g(\vec{k}) = \sum_{\vec{\delta}} e^{i\vec{\delta}\cdot\vec{k}}, \quad (3.32)$$

$$g(\vec{k}) = |g(\vec{k})|e^{i\theta(\vec{k})}. \quad (3.33)$$

$\vec{\delta}$ is the connecting vector between nearest neighbors. For the case of graphene there are three such vectors - $\vec{\delta}_1 = (\frac{a}{\sqrt{3}}, 0)$, $\vec{\delta}_2 = (-\frac{a}{2\sqrt{3}}, \frac{a}{2})$ and $\vec{\delta}_3 = (-\frac{a}{2\sqrt{3}}, -\frac{a}{2})$ - Fig.3.1. The expression for the phase factor $\theta(\vec{k})$ was already derived when the band index $\lambda(\vec{k})$ was investigated. Around the point \vec{k}_F where the energy bands cross the Fermi level it was found that $\theta(\vec{k}) = (-\frac{2\pi}{3} - \tan^{-1} \frac{k_x}{k_y})$ where \vec{k} is small. If the phase factor is included in the $\tilde{B}_{\vec{k}} = B_{\vec{k}}e^{i\theta(\vec{k})}$, H_0 can be diagonalized with the transformation

$$A_{\vec{k}} = \frac{1}{\sqrt{2}}(\alpha_{\vec{k}} + \beta_{\vec{k}}), \quad (3.34)$$

$$\tilde{B}_{\vec{k}} = \frac{1}{\sqrt{2}}(\alpha_{\vec{k}} - \beta_{\vec{k}}), \quad (3.35)$$

$$H_0 = \gamma_0 \sum_n \epsilon_{\vec{k}} [\alpha_{\vec{k}}^+ \alpha_{\vec{k}} - \beta_{\vec{k}}^+ \beta_{\vec{k}}]. \quad (3.36)$$

One of the terms that is produced from the Hamiltonian (eqn.(3.29)) is the modulated hopping that is due to the overlap between two nearest neighboring atoms. In terms of α and β operators

$$\begin{aligned} H_{mod} &= \sum_{\vec{k}, \vec{Q}} [M_{11}(\vec{k}, \vec{Q})(\alpha_{\vec{k}+\vec{Q}}^+ \alpha_{\vec{k}} - \beta_{\vec{k}+\vec{Q}}^+ \beta_{\vec{k}}) \\ &+ M_{12}(\vec{k}, \vec{Q})(\alpha_{\vec{k}+\vec{Q}}^+ \beta_{\vec{k}} - \beta_{\vec{k}+\vec{Q}}^+ \alpha_{\vec{k}})]. \end{aligned} \quad (3.37)$$

But we already have derived this formula in the previous section using different formalism. The result for M_{11} and M_{12} is the same as before. The next step is to take the Fourier transformation of the Coulomb potential

$$\frac{e^2}{|\vec{r}_1 - \vec{r}_2|} = \sum_{\vec{q}} v_q e^{i\vec{q}\cdot(\vec{R}_n - \vec{R}_{n'})}, \quad (3.38)$$

where $v_q = 4\pi e^2/q^2$. Now let the atomic positions be $\vec{R}_n = \vec{R}_n^0 + \vec{u}_n$, where \vec{R}_n^0 is the equilibrium position and \vec{u}_n is a small displacement. We note that in collective

coordinates the number operator is

$$c_n^+ c_n = Z + \frac{1}{N} \sum_{\vec{q} \neq 0} e^{i\vec{q} \cdot \vec{R}_n^0} c_{n, \vec{k} + \vec{q}}^+ c_{n, \vec{k}}. \quad (3.39)$$

Take the Fourier transformation of the electron and ion charge densities. The ions in graphene have $2s$ -wave symmetry. According to [35] the wave function is given by $\psi_{2s} = |c_i| r e^{-\frac{\alpha_i r}{2}}$. The normalization condition gives that $|c_i|^2 = \frac{\alpha_i^5}{96\pi}$. Therefore, using $|c_i|^2$ the Fourier transform of the ion charge density can be easily solved

$$\rho_i(q) = \int d^3r \rho_i(r) e^{i\vec{q} \cdot \vec{r}} = \alpha_i^6 \frac{\alpha_i^2 - q^2}{(\alpha_i^2 + q^2)^4}. \quad (3.40)$$

At the limit of small q the above formula yields

$$\rho_i(q) = \frac{\alpha_i^8}{(\alpha_i^2 + q^2)^4}. \quad (3.41)$$

For the conduction electrons in graphite we take that $\psi_{2p} = |c_e| \vec{r} \cdot \hat{n} e^{-\frac{\alpha_e r}{2}}$ - the free electrons are in $2p_z$ atomic orbitals [35]. To proceed further adopt a coordinate system with z -axis along the q -vector;

$$\begin{aligned} \hat{q} \cdot \hat{r} &= \cos \theta, \\ \hat{q} \cdot \hat{n} &= \cos \theta_0, \\ \hat{r} \cdot \hat{n} &= \cos \theta \cos \theta_0 + \sin \theta \sin \theta_0 \cos \phi. \end{aligned}$$

Thus, the expression for $\rho_e(q)$ becomes

$$\begin{aligned} \rho_e(q) &= |c_e|^2 \int r^4 dr \int_{-1}^1 d(\cos \theta) \\ &\times \int_0^{2\pi} d\phi e^{-\alpha_e r} e^{iqr \cos \theta} [\cos \theta \cos \theta_0 + \sin \theta \sin \theta_0 \cos \phi]^2. \end{aligned} \quad (3.42)$$

One performs the integrations over ϕ and $\cos \theta$ first.

$$\begin{aligned} \rho_e(q) &= 2\pi |c_e|^2 \int r^4 dr e^{-\alpha_e r} [(3 \cos^2 \theta_0 - 1) \\ &\times \left(\frac{1}{qr} \sin qr + \frac{2}{q^2 r^2} \cos qr - \frac{2}{q^3 r^3} \sin qr \right) + \sin^2 \theta_0 \frac{1}{qr} \sin qr]. \end{aligned} \quad (3.43)$$

Now one does the integrals over r and the result is

$$\rho_e(q) = \frac{16\pi|c_e|^2\alpha_e}{(q^2 + \alpha_e^2)^4} [(3 \cos^2 \theta_0 - 1)(\alpha_e^2 - 5q^2) + 3 \sin^2 \theta_0(\alpha_e^2 - q^2)]. \quad (3.44)$$

θ_0 is the angle between \vec{q} and the normal vector to the graphene plane \hat{n} . The normalization of the used $2p_z$ -wave functions determines the constant $|c_e|^2$. One finds $|c_e|^2 = \alpha_e^5/(32\pi)$ and the expression for the electron density turns out to be

$$\rho_e(q) = \frac{\alpha_e^6}{(\alpha_e^2 + q^2)^3}. \quad (3.45)$$

Note that the angle between \vec{q} and the normal vector to the graphite plane is taken to be $\theta_0 = 90^\circ$.

All the preliminary steps in investigating the Hamiltonian from eqn.(3.29) are done. One notices that it is possible to obtain several terms in this way (we already discussed the modulated hopping). One of them is the electron-phonon interaction which is written as

$$\begin{aligned} H_{e-p} &= \frac{i}{\Omega} \sum_{\vec{Q}} X_{\vec{Q}} v_Q \rho_T(Q) \rho_e(Q) \vec{Q} \\ &\cdot [(\hat{\eta}_A e^{i(\theta(\vec{k}-\vec{Q})-\theta(\vec{k}))} + \hat{\eta}_B)(\alpha_{\vec{k}+\vec{Q}}^+ \alpha_{\vec{k}} + \beta_{\vec{k}+\vec{Q}}^+ \beta_{\vec{k}}) \\ &- (\hat{\eta}_A e^{i(\theta(\vec{k}-\vec{Q})-\theta(\vec{k}))} - \hat{\eta}_B)(\alpha_{\vec{k}+\vec{Q}}^+ \beta_{\vec{k}} + \beta_{\vec{k}+\vec{Q}}^+ \alpha_{\vec{k}})] A_{\vec{Q}}, \end{aligned} \quad (3.46)$$

$$X_{\vec{Q}} = \sqrt{\frac{\hbar}{2NM\omega_{\vec{Q}}}}, \quad (3.47)$$

$$A_{\vec{Q}} = a_{\vec{Q}} + a_{-\vec{Q}}^+ \quad (3.48)$$

$$\rho_T(Q) = \rho_i(Q) + Z\rho_e(Q). \quad (3.49)$$

It is the usual form of the linear electron-phonon coupling. The matrix element for transitions within the same band is the term with summation of the polarization vectors of the ions. The one with the difference is the matrix element for transitions between bands. The above formulas are investigated for longitudinal phonons - $\hat{\eta}_{A,B} = \hat{\eta}_{\vec{Q}}$. For graphene only oscillations within the plane are consid-

ered. In the limit of small wave vector \vec{Q} the expressions for the ion and electron densities can be expanded and retaining only the largest terms we find that

$$\tilde{D} = v_Q \rho_T(Q) \rho_e(Q) = 4\pi Z e^2 \left[\frac{3}{\alpha_e^2} - \frac{4}{\alpha_i^2} \right]. \quad (3.50)$$

Therefore, the matrix elements for the electron-phonon interaction are of the form of a deformation potential with a deformation constant given in the above expression. For transitions in the same band and between bands we find

$$M_{11} = 2X_Q \tilde{D} Q_{\perp} \cos\left(\frac{\theta(\vec{k} - \vec{Q}) - \theta(\vec{k})}{2}\right), \quad (3.51)$$

$$M_{12} = 2X_Q \tilde{D} Q_{\perp} \sin\left(\frac{\theta(\vec{k} - \vec{Q}) - \theta(\vec{k})}{2}\right). \quad (3.52)$$

Another type of interaction which is obtained from the original form of the Hamiltonian - eqn.(3.29) - is the direct electron-electron interaction

$$H_{e-e} = \frac{1}{2\Omega} \sum_{\vec{q}} v_q \rho_e^2(q) \rho_A(-\vec{q}) \rho_B(\vec{q}), \quad (3.53)$$

$$\rho_A(q) = A_{\vec{k}+\vec{q}}^+ A_{\vec{k}}, \quad (3.54)$$

$$\rho_B(-q) = e^{i(\theta(\vec{k}-\vec{q})-\theta(\vec{k}))} \tilde{B}_{\vec{k}-\vec{q}}^+ \tilde{B}_{\vec{k}}. \quad (3.55)$$

The integral over q_z can be done and we obtain

$$\begin{aligned} M_{q_{\perp}} &= \int \frac{dq_z}{2\pi} v_q \rho_e^2(q) = 2\pi e^2 \left[\frac{1}{q_{\perp}} - \frac{1}{\sqrt{q_{\perp}^2 + \alpha^2}} \right. \\ &\quad \left. - \sum_{n=1}^{\infty} \frac{(2n-3)!!}{(2n-2)!!} \frac{\alpha^{2n}}{(q_{\perp}^2 + \alpha^2)^{n+1/2}} \right]. \end{aligned} \quad (3.56)$$

Looking at the limit for small q allows the above summation to be truncated. Thus, one takes

$$M_{q_{\perp}} = 2\pi e^2 \left[\frac{1}{q_{\perp}} - \frac{1}{\alpha} \right]. \quad (3.57)$$

Processes between bands and in the same band are possible with the same matrix element.

The last term which we will consider here is a new contribution to the electron-phonon interaction. This is the phonon modulated electron-electron coupling

$$H_{e-ph-m} = -\frac{i}{\Omega} \sum_{\vec{q}, \vec{Q}} \sum_{nn'} X_{\vec{Q}}(\vec{q} \cdot \hat{\eta}_{\vec{Q}}) v_q \rho_e^2(q) \rho_n(\vec{q} + \vec{Q}) \rho_{n'}(-\vec{q}) A_{\vec{Q}}. \quad (3.58)$$

Notice that the above expression is written for $\hat{\eta}_{A,B} = \hat{\eta}_{\vec{Q}}$. Again transitions are possible between different bands. To find what the matrix elements really are for the processes one can perform the summation over n and n' . One finds that there are four possible combinations

$$\begin{aligned} \sum_{nn'=A,B} \rho_n(\vec{q} + \vec{Q}) \rho_{n'}(-\vec{q}) &= \rho_A(\vec{q} + \vec{Q}) \rho_A(-\vec{q}) + \rho_A(\vec{q} + \vec{Q}) \rho_B(-\vec{q}) \\ &+ \rho_B(\vec{q} + \vec{Q}) \rho_A(-\vec{q}) + \rho_B(\vec{q} + \vec{Q}) \rho_B(-\vec{q}). \end{aligned} \quad (3.59)$$

The next thing is to express ρ_A and ρ_B in terms of the α and β operators that diagonalize H_0 . In this way we are able to see that in general processes are possible between any combination of four bands. To determine the matrix elements correctly one needs to put all phase factors which depend on the physical structure of the solid. The complete expression for H_{e-ph-m} for the different transitions is given below.

$$\begin{aligned} H_{e-ph-m} &= -\frac{4i}{\Omega} \sum_{\vec{k}\vec{k}'\vec{q}\vec{Q}} e^{-\frac{\theta_1 + \theta_2}{2}} X_{\vec{Q}}(\vec{q} \cdot \hat{\eta}_{\vec{Q}}) v_q \rho_e^2(q) A_{\vec{Q}} \\ &\times [(\alpha_{\vec{k}+\vec{q}+\vec{Q}}^+ \alpha_{\vec{k}'-\vec{q}}^+ \alpha_{\vec{k}}^- \alpha_{\vec{k}'}^- + \alpha_{\vec{k}+\vec{q}+\vec{Q}}^+ \beta_{\vec{k}'-\vec{q}}^+ \alpha_{\vec{k}}^- \beta_{\vec{k}'}^- + \beta_{\vec{k}+\vec{q}+\vec{Q}}^+ \beta_{\vec{k}'-\vec{q}}^+ \beta_{\vec{k}}^- \beta_{\vec{k}'}^- \\ &+ \beta_{\vec{k}+\vec{q}+\vec{Q}}^+ \alpha_{\vec{k}'-\vec{q}}^+ \beta_{\vec{k}}^- \alpha_{\vec{k}'}^-) \cos \frac{\theta_1}{2} \cos \frac{\theta_2}{2} \\ &- (\alpha_{\vec{k}+\vec{q}+\vec{Q}}^+ \alpha_{\vec{k}'-\vec{q}}^+ \alpha_{\vec{k}}^- \beta_{\vec{k}'}^- + \alpha_{\vec{k}+\vec{q}+\vec{Q}}^+ \beta_{\vec{k}'-\vec{q}}^+ \alpha_{\vec{k}}^- \alpha_{\vec{k}'}^- + \beta_{\vec{k}+\vec{q}+\vec{Q}}^+ \beta_{\vec{k}'-\vec{q}}^+ \beta_{\vec{k}}^- \alpha_{\vec{k}'}^- \\ &+ \beta_{\vec{k}+\vec{q}+\vec{Q}}^+ \alpha_{\vec{k}'-\vec{q}}^+ \beta_{\vec{k}}^- \beta_{\vec{k}'}^-) i \cos \frac{\theta_1}{2} \sin \frac{\theta_2}{2} \\ &- (\alpha_{\vec{k}+\vec{q}+\vec{Q}}^+ \alpha_{\vec{k}'-\vec{q}}^+ \beta_{\vec{k}}^- \alpha_{\vec{k}'}^- + \beta_{\vec{k}+\vec{q}+\vec{Q}}^+ \alpha_{\vec{k}'-\vec{q}}^+ \alpha_{\vec{k}}^- \alpha_{\vec{k}'}^- + \beta_{\vec{k}+\vec{q}+\vec{Q}}^+ \beta_{\vec{k}'-\vec{q}}^+ \alpha_{\vec{k}}^- \beta_{\vec{k}'}^- \\ &+ \alpha_{\vec{k}+\vec{q}+\vec{Q}}^+ \beta_{\vec{k}'-\vec{q}}^+ \beta_{\vec{k}}^- \beta_{\vec{k}'}^-) i \sin \frac{\theta_1}{2} \cos \frac{\theta_2}{2} \\ &- (\alpha_{\vec{k}+\vec{q}+\vec{Q}}^+ \alpha_{\vec{k}'-\vec{q}}^+ \beta_{\vec{k}}^- \beta_{\vec{k}'}^- + \alpha_{\vec{k}+\vec{q}+\vec{Q}}^+ \beta_{\vec{k}'-\vec{q}}^+ \beta_{\vec{k}}^- \alpha_{\vec{k}'}^- + \beta_{\vec{k}+\vec{q}+\vec{Q}}^+ \alpha_{\vec{k}'-\vec{q}}^+ \alpha_{\vec{k}}^- \beta_{\vec{k}'}^-] \end{aligned}$$

$$+ \beta_{\vec{k}+\vec{q}+\vec{Q}}^+ \beta_{\vec{k}'-\vec{q}}^+ \alpha_{\vec{k}} \alpha_{\vec{k}'} \sin \frac{\theta_1}{2} \sin \frac{\theta_2}{2}], \quad (3.60)$$

where

$$\begin{aligned} \theta_1 &= \theta(\vec{k} + \vec{q} + \vec{Q}) - \theta(\vec{k}), \\ \theta_2 &= \theta(\vec{k}' - \vec{q}) - \theta(\vec{k}'). \end{aligned}$$

One notes that the matrix elements in general could be written as a part that is common to all processes and a part that depends on the phase factors. The term that appears in all transitions we denote as

$$|M_{q,Q}| = 4M_q(\vec{q} \cdot \hat{n}_{\vec{Q}})X_{\vec{Q}}, \quad (3.61)$$

$$M_q = v_q \rho_e^2(q). \quad (3.62)$$

Having the formula for the matrix elements one is able to proceed with further calculations.

There have been reports in the literature [32], [33] about electron-electron interaction assisted or mediated by phonons. They investigate a process in which the interaction between two electrons is done by exchanging a phonon. Here the electrons interact through a Coulomb potential, and the distance between the electrons is modulated by the ion vibrations in the solid, which is a different mechanism. This is a new contribution to the ordinary electron-phonon interaction and it is derived for graphite, although the formalism is set for any tight-binding system. Only different phase factors will arise which are different for different solids. Later we show that it can give large contribution to the transport properties compared to the contribution from the modulated hopping.

Chapter 4

Synthesis, Structure and Applications of Single Wall Carbon Nanotubes

4.1 Synthesis of SWNT

Carbon nanotubes are recently discovered nanoscale particles obtained by wrapping layers of graphite into a cylinder. These are a novel class of quasi one-dimensional materials which offer the possibility for new physics and new technology [36]. Although they are built only with carbon atoms, potentially they can be grown in a variety of shapes and sizes. The transport properties are predicted to depend on their geometry.

There are two large groups of carbon nanotubes - multiwall (MWNT) and single wall (SWNT) tubes. As the names show the MWNT are formed by more than one concentric graphite sheet rolled into cylinders with an empty core, and the SWNT are made with only one such a sheet. Most of the observations have been on multiwall carbon nanotubes. The earliest experiments are based on high

resolution transmission electron microscopy on a material produced in a carbon arc. It was shown that there were μm -long tubes with cross sections of several coaxial tubes and a hollow core. Scanning tunneling microscopy and atomic force microscopy have also been used to identify the topological structure of the new materials [9], [10].

A little later SWNTs were also observed. Just like the MWNT they tend to align themselves parallel-like and except for occasional branching they form close-pack bundles or "ropes". The diameter of the rope is maintained constant over the entire length. SWNTs are very flexible. They can bend into curvatures with radii as small as 20 nm. They also have very high tensile strength. One of the largest reported nanotubes is 700 nm long and it has 0.9 nm diameter. The smallest one reported has a diameter only 7 Å. On Fig.4.1 two types of single wall carbon nanotubes are shown.

Since the major interest of this work is the theoretical modeling of the SWNT, we describe only the methods of production of these tubes. They can be produced by the method of carbon arc [2]. Typical synthesis conditions employ voltage of about 20-25 V operating in an inert gas (He) atmosphere with pressure in the range 300-500 Torr. There are two carbon rods (6-7 mm in diameter) which serve the role of a cathode and anode. A hole of about 6 mm is made in the anode. The hole is filled with a mixture of carbon powder and a transition metal (Ni, Co or Fe). The 6 mm diameter cathode rod is pure carbon. A dc current of 95-115 A is passed through the junction. After the arc between the rods is made, they are kept at a distance of 1 mm. The deposit of SWNT starts forming at a rate of about 1 mm/min on the anode while the cathode is consumed. The estimated temperature is 2500-3000 C. The tubes form only where the current flows.

Another technique which is used for producing SWNT is the laser vaporization technique [11]. In contrast to the arc method, this method allows for nanotube production in higher yield and the SWNT are of better quality. The essence of

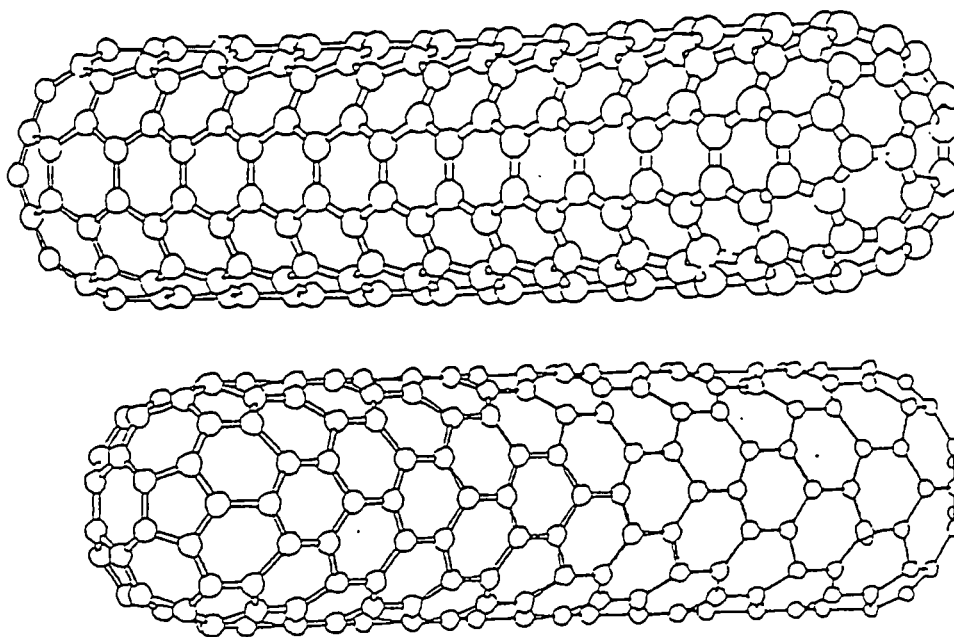


Figure 4.1: Example of two types of SWNT from the many possible tubes

the method is that a scanning laser beam is focused to a 6-7 *mm* in diameter spot in a metal-graphite target. The target is supported in a tube filled with argon atmosphere at a pressure of 500 Torr and heated at a high temperature, thus, the metal-graphite mixture is vaporized and SWNTs are produced. After that the nanotubes are swept by the flowing argon gas and they are deposited on a water-cooled copper collector.

The role of the catalyst for the formation of the tubes is to prevent the carbon pentagons from closing at the growing edge which would be the reason for stopping of the process. To be able to do that the absorption energy of the catalytic particle has to be comparable in strength with the strengths of the carbon bonds, so that the catalytic particle will be held to the carbon structure. In the absence of the catalyst at the tube edge, defects can no longer be annealed efficiently, thus a closure of the growing process will occur.

The produced tubes have a typical diameter of only 14 Å, but can bundle up to form ropes that are as long as tenths of a millimeter. It is not known at present

how much metal catalyst is remained in the tube after the growing is over. It is accepted that large quantities of single wall (10,10) tubes (the meaning of the notation will be explained later) are obtained by these methods. *ab initio* studies also support this conclusion. It is shown in [12] that an armchair (10,10) tube is preferred over a zigzag or any other tube under these experimental conditions.

Therefore, there is a belief that the present methods of catalytic synthesis of single wall tubes produces armchair (which is metallic) tubes with a diameter of 14 Å. Thus, our theoretical investigations will be developed for a one dimensional systems and applied to (10,10) armchair SWNT.

4.2 Applications

Defect-free nanotubes are expected to have remarkable mechanical, as well as electronic and magnetic properties that are in principle tunable by varying the diameter and chirality of the tube. The significance of these nanostructures as electronic materials is the demonstration of quasi-one dimensional wires with a large length-to-diameter ratio, thus, a new field is opening in studying one dimensional physics.

The all-carbon cylindrical molecules (the carbon nanotubes) have proven to have high strength and light weight [14]. This is a very desirable quality for making microscopic devices. Varying the structure along a tube causes varying of the electronic properties. There are some new computer simulations about how the structure of the carbon nanotube is changed if a defect is introduced on the wall [13]. This could be used to make the equivalent of semiconductor junctions which is a basic element of digital electronics.

Devices could be made also as tunnel junctions, or transistors in different circuits, or capacitors. If we have defect-free single wall nanotubes it means that the resulting devices would be very stable to change in the temperature, because the

tubes do not require any doping by impurities, as the conventional semiconductors do. Such transistors and capacitors would have very high intrinsic mobility as well.

Some new studies about chirality-changing in the carbon nanotube due to pentagon-heptagon defects provide a wide range of device possibilities for doped or undoped SWNT [15]. One could arrange the defects along a tube and the electronic structure could be modulated; by putting a defect on the wall of the tube a heterojunction (metal/semiconductor or semiconductor/semiconductor) could be realized. If a doping of the semiconductor side of the metal/semiconductor interface is done then a device similar to a Schottky barrier is available. This is unique because just by removing of a carbon atom a sophisticated device is made.

4.3 Structure of an armchair and zigzag SWNT

Since the calculations will be carried out for one of the highly symmetrical tubes, here we summarize the notation and parameters which will be used later. We start with a layer of graphite. The unit cell was shown in Fig.3.1 where \vec{a}_1 and \vec{a}_2 are the unit vectors.

Their length is $a = \sqrt{3} \times a_{C-C} = 2.46 \text{ \AA}$. To describe a tube it is convenient to specify a chiral vector

$$\vec{C}_h = n\vec{a}_1 + m\vec{a}_2 \quad (4.1)$$

which uniquely determines the shape of the tube. Here n and m are integers. Thus, the tube is named as (n, m) . The pair of integer numbers also completely specifies the chiral angle θ and the diameter d of the tube - Fig.4.2.

If a lattice point O is chosen to be the origin, then any other point can be obtained by the pair of integers (n, m) . By rolling the sheet so that this lattice point coincides with the origin, a tube (n, m) is obtained. Therefore, the pair (n, m) shows that the SWNT can be in almost any shape or size.

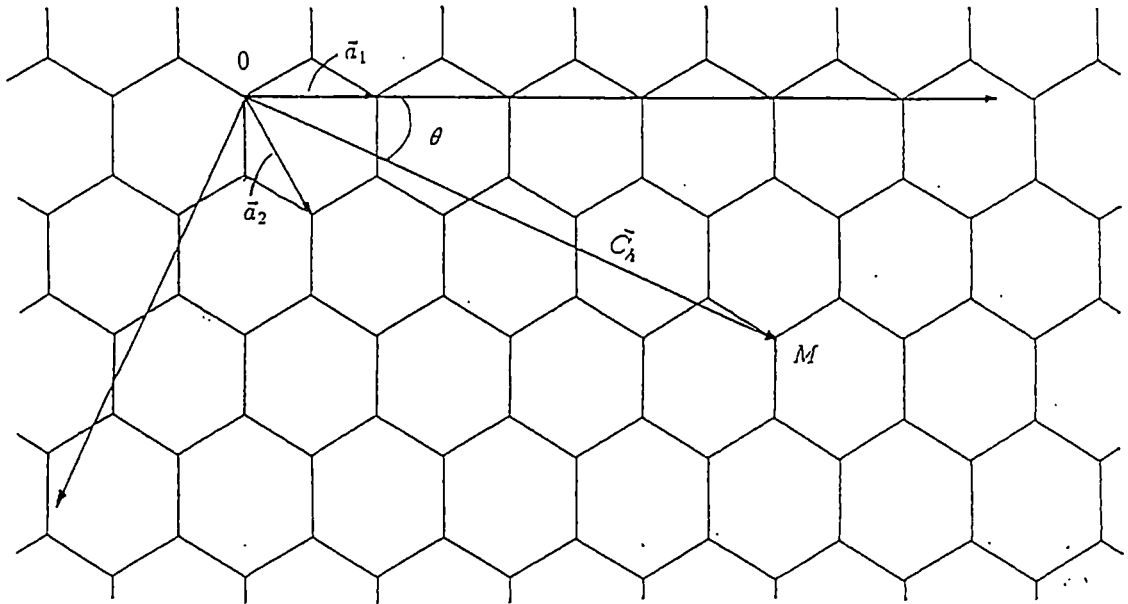


Figure 4.2: An example for a chiral vector is given - $\vec{C}_h = 3\vec{a}_1 + 2\vec{a}_2$. Point M can be mapped into point O by rolling the graphite sheet into a cylinder

The chiral angle θ can be defined to be between the zigzag direction and the vector \vec{C}_h . There are two highly symmetrical cases. One of them is when $n = m$ and the (n, n) tube is called armchair and the other one is when $m = 0$, then the $(n, 0)$ tube is called zigzag. This is shown in Fig.4.3. For an armchair tube $\theta = \frac{\pi}{6}$ and for a zigzag tube $\theta = 0$.

To express the dispersion relations for electrons and phonons in SWNT, it is necessary to specify the unit cell and the basis vectors. For armchair and zigzag tubes, it is convenient to choose a real space rectangular unit cell - Fig.4.4. The area of each real space unit cell contains two hexagons or four carbon atoms. The Brillouin zones are also shown. The corresponding unit cells in reciprocal space has an area n times larger than the area of the corresponding primitive cell in graphene. This large unit cell spans the circumference of the cylinder.

It is predicted by various calculations (from tight-binding approach to *ab initio*) that all armchair tubes will exhibit a metallic behavior. However, for the

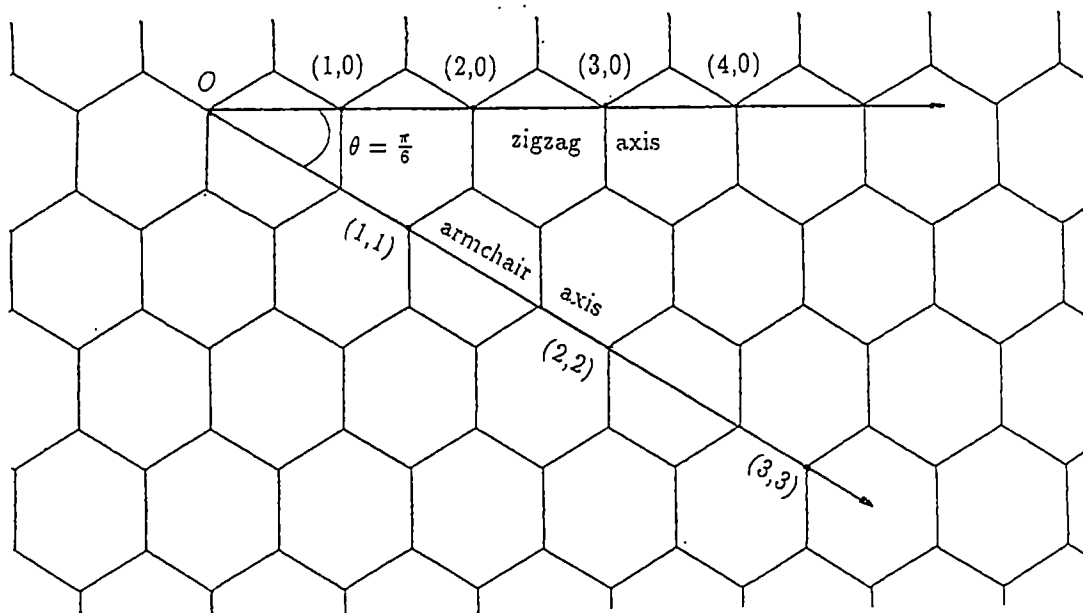


Figure 4.3: The tube axis for the two highly symmetrical cases - zigzag and armchair - are shown.

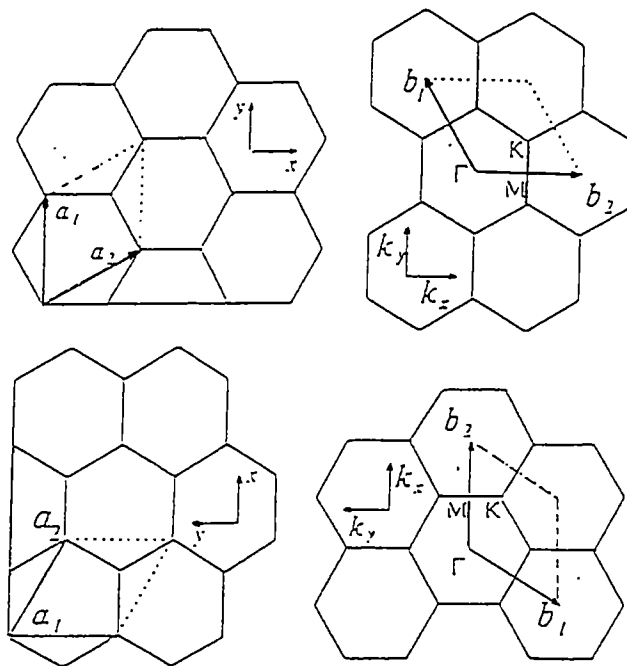


Figure 4.4: a - Brillouin zone for an armchair tube; b - Brillouin zone for a zigzag tube

zigzag tubes only those with n divisible by 3 are metallic and the rest are semi-conducting [16]. Thus, this is a remarkable result - the geometry of these new structures specifies their physical and electronic properties.

Chapter 5

Electron-Phonon Interactions In An Armchair SWNT

5.1 Tight-binding approach

The length of a SWNT is much larger than its diameter. Experiments generally show that the most often observed (10,10) armchair tubes have lengths of the order of a millimeter and the diameter of an individual tube is approximately 14 Å. Thus, this is essentially a quasi one-dimensional system [36], [37].

The whole formalism of describing the carbon nanoparticles was already developed in Ch.3, where we discussed a two dimensional sheet of graphite. An isolated graphene is a semimetal, with the Fermi energy located at a critical point in the two-dimensional π spectrum. For this system, which is closely related to graphene, the Fermi surface is collapsed into one point; there are actually two distinct Fermi points K and K' at $\pm \frac{2\pi}{3a}$ where a is the length of the primitive translational vector, but because of the symmetry of the system we consider only one [38].

The simplest possible method for calculating the effects of electron-phonon

coupling is to utilize the tight-binding approximation for a graphite layer where the curvature of the tube is neglected and boundary conditions around the circumference are applied - a very reasonable approximation for the (10,10) tube [39].

The tube axis for (10,10) tube is along the y -axis on Fig.5.1. This SWNT has 10 hexagons around the circumference. The translational vectors in this coordinate system are

$$\begin{aligned}\vec{a}_1 &= \left(\frac{\sqrt{3}a}{2}, \frac{a}{2}\right), \\ \vec{a}_2 &= \left(\frac{\sqrt{3}a}{2}, -\frac{a}{2}\right).\end{aligned}$$

Thus, we start with the wave functions for graphene given in eqn.(3.1). In the circumferential directions only a finite amount of wave vectors are allowed. The appropriate boundary conditions for an armchair tube are

$$k_x = \frac{m}{N} \frac{2\pi}{\sqrt{3}a}, \quad (5.1)$$

where $m = 0, 2, \dots, N - 1$. The $k_y = k$ wave vector which is along the tube axis is kept continuous.

The wave functions become

$$\psi = \sum e^{i\frac{m}{N}\pi} e^{i(2p+1)\frac{ka}{2}} [f_A + \lambda_{AB} e^{i\frac{m}{N}\frac{2\pi}{3}} f_B], \quad (5.2)$$

where $f_{A,B}$ are the $2p_z$ atomic orbitals centered at the two different atoms in the unit cell.

The energy dispersion relations can also be obtained

$$E = \pm J_0 \left[1 + 4 \cos \frac{m\pi}{N} \cos \frac{ka}{2} + 4 \cos^2 \frac{ka}{2} \right]^{1/2}. \quad (5.3)$$

It is assumed that the overlap integral between nearest neighbors is the same as the one in graphene. The wave vector k is changing in the limits $(-\frac{\pi}{a}, \frac{\pi}{a})$. The constants λ which control the processes between different bands take the form

$$\lambda_{AB} = \pm \frac{e^{-i\frac{m}{N}\frac{2\pi}{3}} (1 + 2e^{i\frac{m}{N}\pi} \cos \frac{ka}{2})}{(1 + 4 \cos \frac{m\pi}{N} \cos \frac{ka}{2} + 4 \cos^2 \frac{ka}{2})^{1/2}}. \quad (5.4)$$

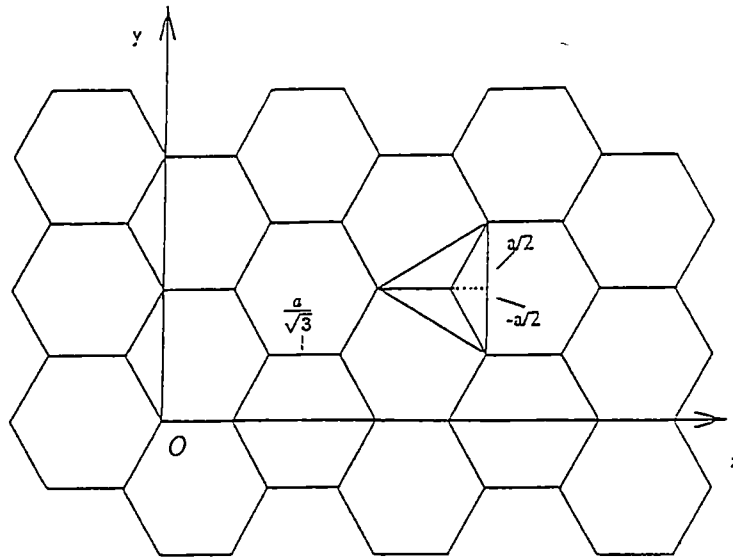


Figure 5.1: x-axis is the zigzag tube axis; y-axis is the armchair tube axis

The resulting calculated energy bands for (10,10) tube are presented in Fig.5.2. One sees that there are 20 conduction and 20 valence bands. Two of them are nondegenerate and they cross the Fermi level at points $\pm \frac{2\pi}{3a}$. The others are doubly degenerate. This is a result common to all armchair tubes - there are always $2n$ conduction bands and $2n$ valence bands and the two nondegenerate ones cross the Fermi level. Thus, an armchair tube is expected to be a metal - only infinitesimal excitations are needed to excite carriers into the conduction band.

The reason for that has a quantum mechanical nature and it is based on the electronic structure of two dimensional graphite with π bands degenerate at the K points of the hexagonal Brillouin zone. The periodic boundary conditions for the one dimensional tube permit only a finite number of wave vectors to exist around the circumference and since at least one of them passes through the K point for an armchair SWNT, it is expected to have a metallic behaviour.

Again we are interested in carrier excitations around the K points in the Brillouin zone. The boundary condition for the discrete wave vector for these two

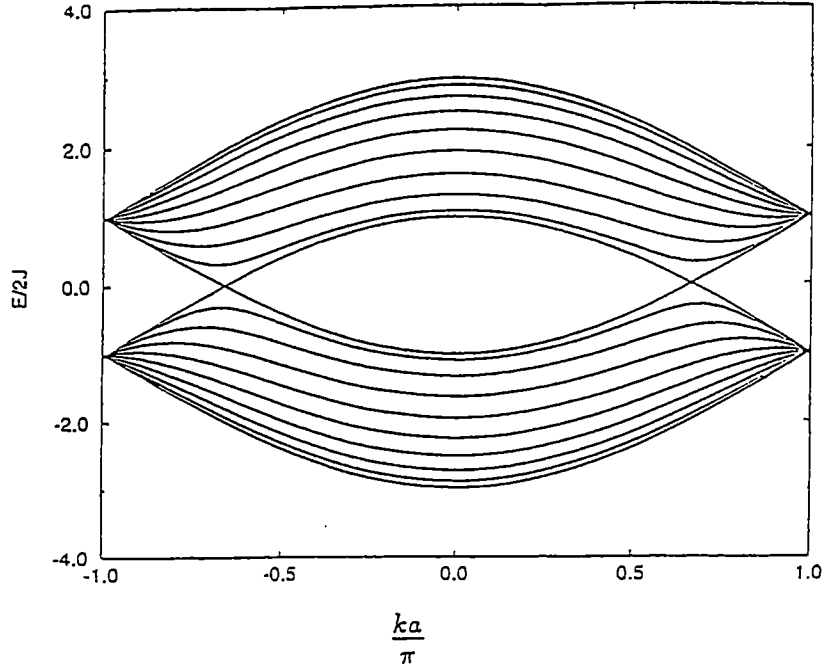


Figure 5.2: Energy bands for an infinitely long (10,10) armchair carbon nanotube

bands reads

$$k_x = \frac{2\pi}{\sqrt{3}a}. \quad (5.5)$$

The continuous wave vector, which is along the tube axis, can be expanded around the crossing point. Thus, instead of k we substitute $k_0 + \tilde{k}$ where $k_0 = \frac{2\pi}{3a}$ and \tilde{k} is small.

After the expansion around k_0 the energy dispersion relation for the two lowest bands takes the form

$$E = \pm v_F \tilde{k}, \quad (5.6)$$

where $v_F = J_0 \frac{\sqrt{3}a}{2}$. As in graphene one obtains a linear k dependence in the energy with the difference that k is a one dimensional vector (\tilde{k} is renamed back to k).

The constants λ are

$$\lambda_{1,2} = \pm e^{-i\frac{2\pi}{3}}. \quad (5.7)$$

It is interesting to note that they do not depend on the wave vector which follows

from the symmetry of the system.

We start by examining the modulated hopping of the electron-phonon interaction in an armchair SWNT. This type of coupling plays an important role in the transport processes of the tube. In fact, the electron-phonon coupling is the deciding factor for the values of the transport properties for most metallic systems at higher temperatures. The formalism was already developed for graphene. All one needs to do is to convert the problem into a one dimensional one by applying the appropriate boundary conditions [40]. The form of the Hamiltonian for the interaction is the same as before

$$H_{int} = \sum M_{kk+Q,\lambda^i\lambda^j} c_{k+Q,\lambda^i}^+ c_{k,\lambda^j} (b_Q + b_{-Q}). \quad (5.8)$$

The evaluation of the matrix elements are based on the matrix elements for graphene, given in eqns.(3.21-3.24). λ^i and λ^j are the band indices. The summations over nearest neighbors are done and the expressions simplify to

$$\begin{aligned} M_{kk+Q,11} &= 2q_0 J_0 X_Q [(\eta_{Ax} - \eta_{Bx})(1 + \cos \frac{Qa}{4} \cos(\frac{\pi}{3} + \frac{Qa}{4})) \\ &+ \sqrt{3}i(\eta_{Ay} + \eta_{By}) \sin \frac{Qa}{4} \cos(\frac{\pi}{3} + \frac{Qa}{4})], \end{aligned} \quad (5.9)$$

$$\begin{aligned} M_{kk+Q,12} &= 2q_0 J_0 X_Q [i(\eta_{Ax} + \eta_{Bx}) \sin \frac{Qa}{4} \sin(\frac{\pi}{3} + \frac{Qa}{4}) \\ &+ \sqrt{3}(\eta_{Ay} - \eta_{By}) \cos \frac{Qa}{4} \sin(\frac{\pi}{3} + \frac{Qa}{4})]. \end{aligned} \quad (5.10)$$

Notice that the phase factor ϕ does not exist here any more. The reason is the quasi-one dimensionality of the system. By \vec{k} we mean that $k_x = \frac{2\pi}{\sqrt{3}a}$ is quantized in units and $k_y = k$ is the continuous variable. These are the exact expressions for the electron-phonon coupling for the (10,10) SWNT.

5.2 Deformation potential approximation

Further insight can be gained by looking at the deformation potential approximation. It was discussed for graphene. Here we do the same for SWNT. We

expect to find many similarities between the two. The reason why we consider the deformation potential approach is that the electronic states are around the Brillouin zone edge near the K -point. Taking the limit of a small wave vector k around the K - point and a small phonon vector Q the matrix elements become

$$M_{11} = 2q_0J_0X_Q\left[\frac{3}{2}(\eta_{Ax} - \eta_{Bx}) + (\eta_{Ay} + \eta_{By})i\frac{\sqrt{3}}{8}Qa\right], \quad (5.11)$$

$$M_{12} = 2q_0J_0X_Q\left[(\eta_{Ax} + \eta_{Bx})i\frac{\sqrt{3}}{8}Qa + \frac{3}{2}(\eta_{Ay} - \eta_{By})\right]. \quad (5.12)$$

As it was found in graphene, not only the longitudinal modes matter, but also the optical phonons should be taken into account. This is done by using the results from Ch.2. Thus, the final form for the matrix elements for the modulated hopping is

$$M_{11} = q_0J_0X_Q\frac{\sqrt{3}}{4}Qa(\eta_{Ay} + \eta_{By})(1 - R), \quad (5.13)$$

$$M_{12} = q_0J_0X_Q\frac{\sqrt{3}}{4}Qa(\eta_{Ax} + \eta_{Bx})(1 - R). \quad (5.14)$$

Due to the optical modes the matrix elements are reduced by R which depends on the parameters α and β - the constants which characterize the phonon spectrum for the tube. Since $(1 - R) \sim 0.33$ then squaring the matrix element causes a significant reduction of $(1 - R)^2 \sim 0.1$.

Both processes - interband and intraband - have a deformation type of potential. Following the convention, it is useful to represent the Hamiltonian of the interaction in the form

$$H = D \sum_{kQ} X_Q Q c_{k+Q,\lambda}^+ c_{k,\lambda} (b_Q + b_{-Q}^+), \quad (5.15)$$

where $D = \frac{\sqrt{3}}{2}q_0J_0a$ is the deformation potential constant and it is the same for both types of processes.

The message from this calculation is that the geometrical structure of the metallic armchair SWNT is manifested in the matrix elements controlling the

electron-phonon interaction. We believe that the topology of the tube plays an essential role in all transport processes. Thus, the gapless carrier excitations about the critical points should be examined very carefully. As it was obtained for graphene, not only the longitudinal modes are important, but also the transverse modes are. We also have found that the transitions in the same band are controlled by the longitudinal phonons and the processes between bands are controlled by the transverse phonons.

Compare with the results from ref. [40]. It can be seen that both calculations give similar results about the dependance on the phonon wave vector Q . The major difference is that the matrix elements here are shown to be reduced by a factor $(1 - R)$ because of the coupling between the acoustic and optical phonons. This was not found in [40] and we consider the above results as improvement.

5.3 Electron-phonon and phonon-modulated electron-electron interactions

Many similarities are expected between a SWNT and a sheet of graphite. In the chapter about graphene we looked beyond the traditional modulated hopping for graphene. New terms arise to the electron-phonon interaction which could give appreciable contributions. Later we will show that these effects can be important in the transport properties of the carbon nanoparticles. Once again we expect the symmetry of the system to play an essential role.

All the formulas developed previously for the two dimensional graphite layer are expected to be valid here. We need only impose discrete boundary conditions for our case and make the transformation from a two dimensional solid into a one dimensional one.

One notices that the expressions for the electron charge density and ion charge density are the same as for graphene.

Consider the electron-phonon interaction. The Hamiltonian has the same form as in eqn.(3.46) from Chapter about graphene. Now the phonon wave vector \vec{Q} is taken to be along the tube axis and only acoustic modes are of interest. The deformation constant \tilde{D} is also the one derived for graphene. Thus, because of the modulation of the bare Coulomb potential due to $\rho_T(Q)$ and $\rho_e(Q)$ the electron-phonon interaction is of deformation type.

The phase factor $\theta(\vec{k})$ is also involved in the expression for the matrix elements. For a (10,10) SWNT it was already derived that it is a constant $\theta(\vec{k}) = -2\pi/3$. Therefore,

$$M_{11} = -iX_{Q_z}\tilde{D}Q_z, \quad (5.16)$$

$$M_{12} = f(Q_z^2). \quad (5.17)$$

An interesting result is obtained here - transitions between two different bands to first order of the phonon wave vector are not allowed in the armchair tube. In Ch.2 we have derived that the optical phonons are connected to the acoustic phonons. The coefficients of proportionality contain Q . Thus, $M_{12} \sim Q^2$. This is another manifestation of the symmetry and one-dimensionality of the system. Another thing that is noticed is that the matrix elements for intraband transitions display a deformation type of approximation with a deformation constant \tilde{D} as it was found for graphene.

Another term which was obtained from the general Hamiltonian set for graphene is the ordinary electron-electron interaction. We notice that the integration over Q_\perp can be done. Thus, the matrix elements for transition between any combination of bands up to a phase factor take the form

$$\begin{aligned} M_{q_z} &= \int \frac{d^2 q_\perp}{(2\pi)^2} v_q \rho_e^2(q) = 2e^2 \left[\ln \frac{\pi q_z}{2k_F} - \ln \frac{\pi}{2k_F} \sqrt{q_z^2 + \alpha^2} \right. \\ &\quad \left. + \sum_{n=2}^6 \frac{(2n-3)!!}{(2n-2)!!} \frac{\alpha^{2n}}{(Q_z^2 + \alpha^2)^n} \right], \end{aligned} \quad (5.18)$$

$$M_{q_z} \approx 2e^2 \ln \frac{q_z}{\alpha}. \quad (5.19)$$

At small q_z the last expression is a reasonable approximation for the matrix element of the Coulomb interaction.

And the last term which was investigated for graphene is the phonon modulated electron-electron coupling. This is actually the new contribution to the electron-phonon interaction and comes from the modulation of the distance between two electrons in the Coulomb potential due to the lattice vibrations. We obtain the matrix elements by looking at eqn.(3.60) from Ch.3. One notices that for the tube $\theta_1 = 0$ and $\theta_2 = 0$ because the phase factors are constants. Therefore, only the first term in eqn.(3.60) survives and the matrix element up to a phase factor is given by the expression

$$M_{q_z, Q_z} = -4iM_{q_z}(\vec{q} \cdot \hat{\eta}_{\vec{Q}})X_{Q_z}. \quad (5.20)$$

The different matrix elements corresponding to different electron-phonon coupling processes are obtained. Thus, one is able to proceed further with investigation of the effects following from these transitions on the characteristics of two dimensional graphite and a quasi-one dimensional (10,10) SWNT. The expressions for the different terms in the original Hamiltonian - eqn.(3.29) - is rather general and it can be applied to other tight-binding systems. The idea is that the effects of several contributions with different origin are comparable for low dimensional systems and the evaluation of the transport characteristics needs to be done carefully.

The geometry of a certain solid comes into play when one puts all the phase factors. Also the ion and electron charge densities are different for different solids. The differences are not only in the constants $\alpha_e, \alpha_i, |c_e|$ and $|c_i|$, but also in the type of wave symmetry of the ions and electrons.

If one wants to simplify the calculation further, one can neglect the modulation terms in the expression for M_{q_z} and take only the unscreened Coulomb potential

in 1D. For small wave vectors $q_z \ll \alpha$ the bare Coulomb potential is a good approximation.

Notice that the above was done assuming that this is essentially a one-dimensional system. But carbon nanotubes have finite diameters and we consider them being quasi-one dimensional. Thus, if one needs to be more precise this should be taken into account [41]. Thus, the Coulomb interaction for electrons on a cylinder with radius R is modified to

$$M_{qQ} = \alpha' I_L(qR) K_L(qR) \sqrt{\frac{\hbar}{2NM\omega_Q}} i(\vec{q} \cdot \hat{\xi}_Q). \quad (5.21)$$

$I_L(qR)$ and $K_L(qR)$ are the modified Bessel functions from first and second kind of the order L - which stands for angular momentum of the interaction. If $L = 0$ then we are dealing with a intraband transitions; if $L = 1$ then the transitions are interband. But in our transitions between bands do not take place and therefore L is always zero.

Chapter 6

Electron Self-Energy

6.1 Modulated hopping and linear electron-phonon interaction

The imaginary part of the electron self-energy is a very important quantity. It is closely related to the relaxation time of the electrons. Thus, several transport properties depend on the self-energy. In this chapter we will examine the impact of different types of interactions on it.

The first effect which will be discussed is how the imaginary part of the self-energy depends on the electron-phonon interaction. The basic diagram is given on Fig.6.1. It has one phonon line represented by a dashed line.

The expression for the self-energy is well-known and in the high temperature limit is given by [30]

$$-Im\Sigma(\vec{k}) = 2\pi(k_B T) \sum_{\vec{Q}} \frac{|M_{\vec{Q}}|^2}{\hbar\omega_Q} \delta(\epsilon_{\vec{k}} - \epsilon_{\vec{k}+\vec{Q}}). \quad (6.1)$$

Thus, we obtain that the $-Im\Sigma(\vec{k})$ is proportional to the temperature T . At this

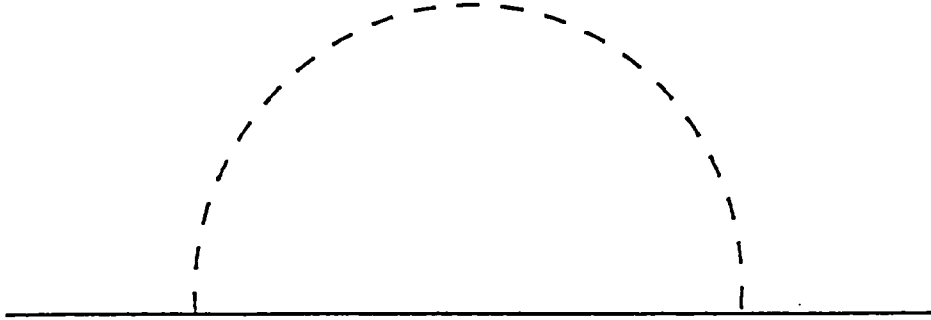


Figure 6.1: Diagram for the first order electron-phonon interaction

stage one can define the following quantity

$$\lambda = 2 \sum_{\vec{Q}} \frac{|M_{\vec{Q}}|^2}{\hbar\omega_Q} \delta(\epsilon_{\vec{k}} - \epsilon_{\vec{k}+\vec{Q}}). \quad (6.2)$$

λ is dimensionless and it represents the coupling constant of the appropriate interaction.

There are two types of electron-phonon interaction for the low dimensional tight-binding systems which are in consideration here - modulated hopping and linear electron-phonon interaction. The above diagram describes both of them. The only difference which will have an impact on further estimations is in the matrix elements.

Consider the quasi-one dimensional armchair SWNT. The matrix elements for the modulated hopping were already calculated and they display a deformation type of potential. The energy dispersion is also known - $\epsilon_k = \pm J_0[1 - 2 \cos \frac{ka}{2}]$.

Therefore, using the properties of the δ -function we find

$$\lambda_{ij} = \frac{|D|^2 L_0}{8\pi\alpha} \int dQ \frac{Q^2}{\sin^2 \frac{\pi Q}{2q_D}} \delta(\epsilon_k^i - \epsilon_{k+Q}^j) = \frac{|D|^2 k_F}{2\pi\alpha v_F}, \quad (6.3)$$

where the band indices are $i, j = 1, 2$, D is the deformation constant, L_0 is the length of the unit cell in 1D and α is the spring constant of the solid. We have defined it in Ch.2. The above formula is the same for transitions in the same band and between bands. The reason is that the energy dispersion is linear with the wave vector and that the electron energy has an opposite sign of the hole energy.

The essence from the above result is that due to the facts that the energy dispersion is linear and the solid is one dimensional, it follows that only excitations between the two bands - Fig.6.2 - contribute to the coupling constant of the modulated hopping.

Notice that we have made use of the following model

$$\rho\omega_Q^2 = \frac{4\alpha}{L_0} \sin^2 \frac{\pi Q}{2q_D}, \quad (6.4)$$

where ρ is the mass density and α is the spring constant. q_D is the radius of the Debye sphere.

The same procedure is applied for the linear electron-phonon interaction. One is interested only in transitions between the two bands - Fig.6.2. But it was found that the matrix element for this kind of processes was zero. Therefore, it follows that the ordinary electron-phonon coupling does not have any impact on the $-Im\Sigma(\vec{k})$.

For graphene similar results can be obtained. The only difference is that now \vec{Q} is two-dimensional and the integration is over two variables. The δ -function is used to do the integration over the ϕ variable

$$\lambda = \frac{|D|^2 A_0}{16\pi^2 \alpha v_F} \int dQ \frac{Q^2}{\sin^2 \frac{\pi Q}{2q_D}} = \frac{2|D|^2 q_D}{\pi^4 \alpha v_F} \times I_1, \quad (6.5)$$

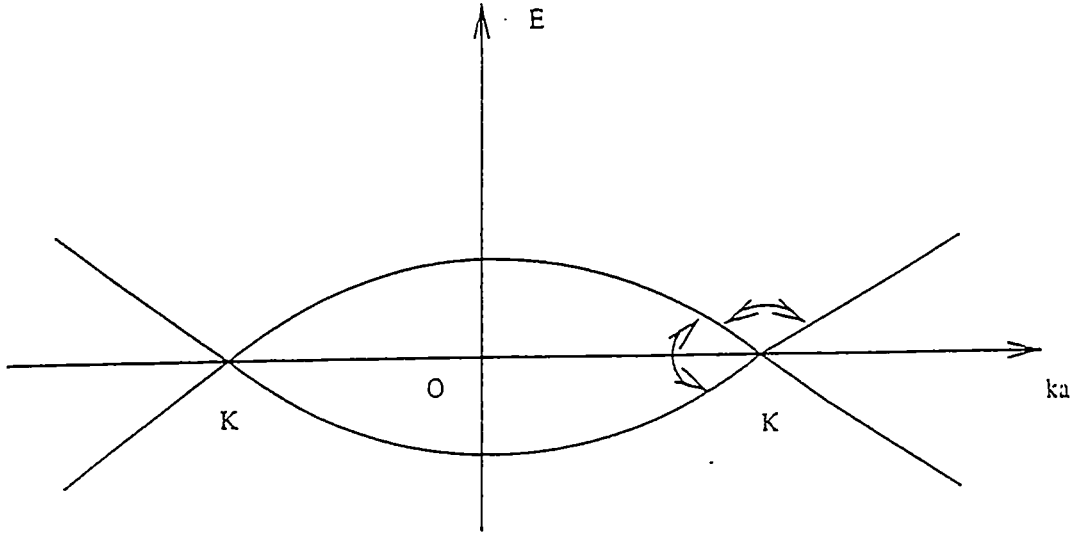


Figure 6.2: Only the two lowest bands that cross the Fermi level at the Brillouin zone edge are of interest.

where the q_D is the radius of the Debye circle in 2D for a hexagonal lattice (Fig.3.1)

$$\pi q_D^2 = \frac{(2\pi)^2}{A_0} \quad (6.6)$$

$$A_0 = \frac{\sqrt{3}}{2} a^2. \quad (6.7)$$

Thus, for the integral I_1 it is easy to find

$$I_1 = \int_0^{\pi/2} dx \frac{x^2}{\sin^2 x} \approx 2.18. \quad (6.8)$$

Notice that both intraband and interband processes contribute to λ with the same magnitude.

To derive an expression for λ for the linear electron-phonon interaction in graphene it is enough to replace D with \tilde{D} in eqn.(6.3) and eqn.(6.5); the result could have been written by inspection. Processes between different bands are possible with the appropriate substitution for \tilde{D} .

6.2 RPA for the phonon modulated Coulomb interaction

6.2.1 Derivation of the Imaginary part of the electron self-energy

Here the main objective is to treat the problem in terms of the new type of interaction - the phonon modulated electron-electron interaction. We already have written the form of its Hamiltonian. In this chapter we investigate the impact of it on the transport properties of the electrons in an armchair SWNT and graphene. The model is that every atom in the system has conduction electrons and the average charge on each atom is zero. In deriving of this Hamiltonian we assumed that the rigid ion approximation is valid, thus, the electrons follow the motion of the ions in the process of phonon vibrations. It is found that this type of interaction has interesting results in lower dimensions.

In order to understand that we look at the matrix elements for graphene and for a SWNT given in eqns.(3.60) and (5.20). For small wave vectors v_q is taken to be the ordinary Coulomb interaction in 1D and 2D which we will assume to be true for easier estimates. At larger values of q the matrix element is modulated in a complicated way.

Next the electron self-energy is calculated in the one-phonon approximation. The Feynman diagram is shown in Fig.6.3a. There are two Coulomb lines represented by wiggly lines. The dashed line is the phonon line. Higher order diagrams are shown in Fig.6.3b. The summation of the self-energy terms from Fig.6.3b is the random phase approximation (RPA) with one phonon line.

To evaluate the self-energy we start with the lowest order in the S -matrix expansion [30]

$$\begin{aligned}
 \mathcal{G}(\vec{p}, \tau - \tau') &= \frac{1}{2} M_{q_1 Q_1} M_{q_2 Q_2} \int d\tau_1 d\tau_2 \langle T_\tau c_{\vec{p},j}(\tau) c_{\vec{k}_1 + \vec{q}_1 + \vec{Q}_1, l}^+(\tau_1) \\
 &\times c_{\vec{k}'_1 - \vec{q}_1, m}^+(\tau_1) c_{\vec{k}_1, l}(\tau_1) c_{\vec{k}'_1, m}(\tau_1) c_{\vec{k}_2 + \vec{q}_2 + \vec{Q}_2, r}^+(\tau_2) c_{\vec{k}'_2 - \vec{q}_2, r}^+(\tau_2) \\
 &\times c_{\vec{k}_2, n}(\tau_2) c_{\vec{k}'_2, r}(\tau_2) c_{\vec{p}, j}^+(\tau') \rangle \langle T_\tau A_{\vec{Q}_1}(\tau_1) A_{\vec{Q}_2}(\tau_2) \rangle . \quad (6.9)
 \end{aligned}$$

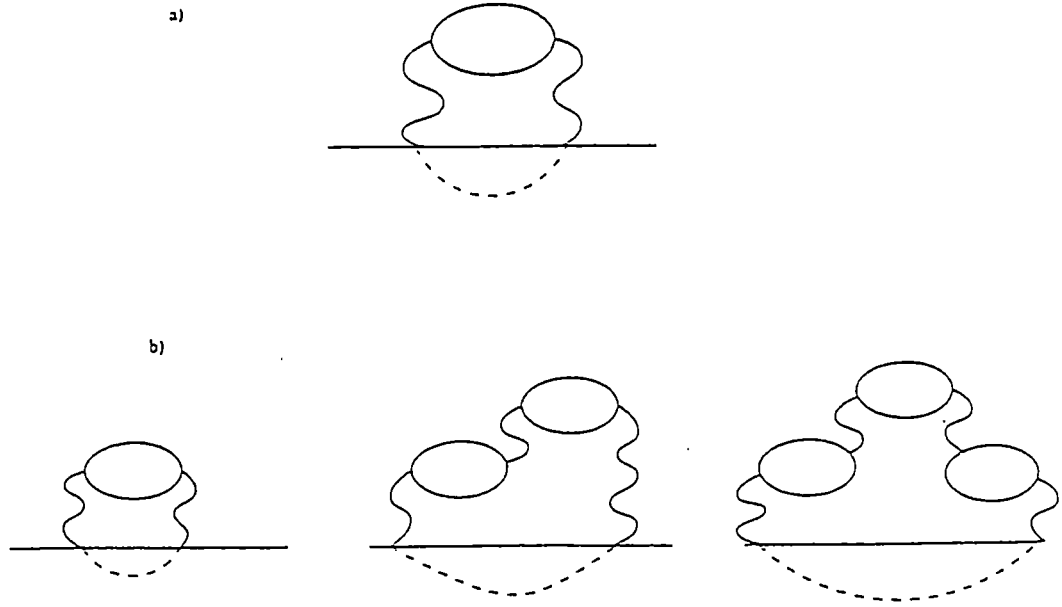


Figure 6.3: a - Feynman diagram with two Coulomb lines and one phonon line; b - RPA with one phonon line

Here j, l, m, n, r are band indices and they take values 1 and 2 only. The diagram for which the above expression is written is the one from Fig.6.3a. Also the standard substitution for $A_{\vec{Q}}$ is used

$$A_{\vec{Q}} = a_{\vec{Q}} + a_{-\vec{Q}}^+ \quad (6.10)$$

First one notices that there are several possible combinations involving different band indices. Then there are several possible combinations for the Coulomb and phonon wave vectors which arise from the different pairings of the electron operators in the above equation. For the phonon wave vectors one obtains

$$\vec{Q}_1 = \vec{Q}_2 \quad (6.11)$$

and then the combinations for the \vec{q} -vectors are

$$\vec{q}_2 = \vec{q}_1, \quad (6.12)$$

$$\vec{q}_2 = -\vec{q}_1 - \vec{Q}, \quad (6.13)$$

$$\vec{q}_2 = -\vec{q}_1 + \vec{Q}. \quad (6.14)$$

Note that adding together these different possibilities changes the factor of $(\hat{\eta}_{\vec{Q}} \cdot \vec{q}_1)(\hat{\eta}_{\vec{Q}} \cdot \vec{q}_2)$ into $(\hat{\eta}_{\vec{Q}} \cdot \vec{Q})^2$. To obtain the RPA correlation energy of the electron gas one needs to perform the frequency summations of the summed diagrams from Fig.6.3b

$$\begin{aligned} \Sigma(\vec{k}) &= \frac{\hbar}{2NM\beta^2} \sum_{iq_n iQ_n} \sum_{\vec{q}\vec{Q}} \frac{(\hat{\eta}_{\vec{Q}} \cdot \vec{Q})^2}{\omega_Q} \mathcal{D}^0(\vec{Q}, iQ_n) \\ &\times \mathcal{G}^0(\vec{k} + \vec{Q} + \vec{q}, ik_n + iQ_n + iq_n) \frac{M_q^2 P_q}{1 - M_q P_q}, \end{aligned} \quad (6.15)$$

where P_q is the polarization factor of each bubble

$$P_q = 2 \int \frac{d^3k}{(2\pi)^3} \frac{f_{\vec{k}} - f_{\vec{k}+\vec{q}}}{iq_n + \epsilon_{\vec{k}} - \epsilon_{\vec{k}+\vec{q}}}. \quad (6.16)$$

We try to obtain some general results in order to receive an idea about the problem. In doing the summations over Matsubara frequencies one has to do the summations before performing any analytical continuations such as substituting $ik_n \rightarrow \epsilon_k + i\delta$.

We proceed with the summation over iQ_n and the result is

$$\begin{aligned} \Sigma(\vec{k}) &= \frac{\hbar}{2NM\beta} \sum_{iq_n} \sum_{\vec{q}\vec{Q}} \frac{(\hat{\eta}_{\vec{Q}} \cdot \vec{Q})^2}{\omega_Q} \frac{M_q^2 P_q}{\epsilon_{RPA}} \left[\frac{N_Q + f''}{iq_n + ik_n + \omega_Q - \epsilon''} \right. \\ &\left. + \frac{1 + N_Q - f''}{iq_n + ik_n - \omega_Q - \epsilon''} \right], \end{aligned} \quad (6.17)$$

where the following definitions are made

$$\begin{aligned} \epsilon_{RPA} &= 1 - M_q P_q, \\ \epsilon'' &= \epsilon_{\vec{k}+\vec{q}+\vec{Q}}, \\ N_Q &= 1/(e^{\beta\epsilon_k} - 1), \\ f'' &= 1/(e^{\beta\epsilon''} + 1). \end{aligned}$$

Now one needs to do the summation over iq_n . Unfortunately, the function under the integral contains complicated arguments, so that the integral in most cases will need to be done numerically. But for certain "simple" systems (as we show later) we can find analytical expressions.

To continue further with the problem one can employ Lehmann representation

$$\Sigma(\vec{k}) = \frac{\hbar}{2NM} \sum_{\vec{Q}} \frac{(\hat{\eta}_{\vec{Q}} \cdot \vec{Q})^2}{\omega_{\vec{Q}}} \mathcal{D}^0(\vec{Q}, iQ_n) \int \frac{d\epsilon''}{2\pi} \frac{A(\vec{k} + \vec{Q}, \epsilon'')}{ik_n + iQ_n - \epsilon''}, \quad (6.18)$$

where $A(\vec{k} + \vec{Q}, \epsilon'')$ is the spectral function for the electron self-energy. Now the summation over iQ_n is done and one obtains

$$\begin{aligned} \Sigma(\vec{k}) &= \frac{\hbar}{2NM} \sum_{\vec{Q}} \frac{(\hat{\eta}_{\vec{Q}} \cdot \vec{Q})^2}{\omega_{\vec{Q}}} A(\vec{k} + \vec{Q}, \epsilon'') \left[\frac{N_{\vec{Q}} + f''}{ik_n + \omega_{\vec{Q}} - \epsilon''} \right. \\ &\quad \left. + \frac{1 + N_{\vec{Q}} - f''}{ik_n - \omega_{\vec{Q}} - \epsilon''} \right]. \end{aligned} \quad (6.19)$$

In the high temperature limit the imaginary part of the self-energy is

$$\begin{aligned} -Im\Sigma(\vec{k}) &= \frac{k_B T}{NM(2\pi)^3} \int d^3Q \frac{(\hat{\eta}_{\vec{Q}} \cdot \vec{Q})^2}{\omega_{\vec{Q}}^2} [A(\vec{k} + \vec{Q}, \epsilon - \omega_Q) \\ &\quad + A(\vec{k} + \vec{Q}, \epsilon + \omega_Q)]. \end{aligned} \quad (6.20)$$

When the wave vector \vec{k} is near the Fermi surface the spectral function could be written as [43]

$$A(\vec{k} + \vec{Q}, \epsilon \pm \omega_Q) = F(\vec{k} + \vec{Q})(\epsilon - \epsilon_F \pm \omega_Q)^2. \quad (6.21)$$

The difference $\epsilon - \epsilon_F$ vanishes at the Fermi surface. Thus, one arrives at

$$-Im\Sigma(\vec{k}) = \frac{k_B T}{NM(2\pi)^3} \int d^3Q F(\vec{k} + \vec{Q}). \quad (6.22)$$

Two things should be noticed here. First, the imaginary part of the self-energy is proportional to T - a typical result for the ordinary electron-phonon interaction.

Second, the ion mass is still in the denominator, which means that this term can be considered small. Thus, the general idea and conclusion are that the types of diagrams shown in Fig.6.3 are not expected to play a significant role in the transport processes governed by the phonon-modulated electron-electron interaction.

6.2.2 RPA for the armchair SWNT

Some analytical results for the RPA diagrams are possible to be obtained for SWNT which is an example of a quasi-one dimensional system. The reason is the following: Only excitations in the two lowest energy bands are considered. They cross the Fermi level at the K points in the Brillouin zone and the energy dispersion is linear with the wave vector - $\epsilon = \pm v_F(k - k_F)$ where v_F is the Fermi velocity and the wave vector k is changing from $-k_F$ to k_F . In this model the integrals in eqn.(6.17) can be evaluated. Although the model is the same for graphene, one is not able to obtain closed form results because the problem is two-dimensional.

Note that the expression for P_q from eqn.(6.16) is for a one band model. Here excitations are possible between two bands. Using the fact that $f(-x) = 1 - f(x)$ for the Fermi distribution function including all types of excitations one is able to arrive at

$$P_q = 2 \int \frac{dk}{2\pi} [(f_k - f_{k-q}) \frac{2(\epsilon_k - \epsilon_{k-q})}{(\epsilon_k - \epsilon_{k-q})^2 - (iq_n)^2} - (1 - f_k - f_{k-q}) \frac{2(\epsilon_k + \epsilon_{k-q})}{(\epsilon_k + \epsilon_{k-q})^2 - (iq_n)^2}], \quad (6.23)$$

where

$$\begin{aligned} \epsilon_k - \epsilon_{k-q} &= v_F q, \\ \epsilon_k + \epsilon_{k-q} &= 2v_F k_F + 2v_F k - v_F q. \end{aligned}$$

The first term in eqn.(6.23) comes from intraband interactions and the second one comes from interband interactions. The integration can be easily done using the fact that the Fermi distribution function is a step function at zero temperature (Appendix I). The result is

$$P_q = \frac{v_F q^2}{\pi((v_F q)^2 - (iq_n)^2)} + \frac{2}{\pi v_F} \ln \frac{(4v_F k_F)^2 - (iq_n)^2}{(v_F q)^2 - (iq_n)^2}. \quad (6.24)$$

Both terms in the above expression have poles at $\pm v_F q$. Since we are interested in the limit of $q \rightarrow 0$ the logarithmic term can be neglected as having a much weaker divergence compared to the first one. It seems like the excitations for small wave vectors from the electron-hole band transitions have little effect on the polarization factor in this 1D system. Only the intraband transitions are important [44]. Therefore,

$$P_q = \frac{v_F q^2}{\pi((v_F q)^2 - (iq_n)^2)}, \quad (6.25)$$

$$\epsilon_{RPA} = 1 + \frac{v_F M_q q^2 / \pi}{(iq_n)^2 - (v_F q)^2}. \quad (6.26)$$

To obtain the correct result for the electron self-energy all of the frequency summations have to be done before making the continuation $ik_n \rightarrow \epsilon_k + i\delta$. The summation over iq_n can be easily performed in eqn.(6.17)

$$\begin{aligned} \Sigma(\vec{k}) = & \frac{\hbar v_F}{NM\pi} \sum_{qQ} \frac{(\hat{n}_Q \cdot \vec{Q})^2 q^2 M_q^2}{\omega_Q M_q'} \left[\frac{N(M_q') + f(\epsilon'' - \omega_Q)}{ik_n + M_q' + \omega_Q - \epsilon''} \right. \\ & + \frac{1 + N(M_q') - f(\epsilon'' - \omega_Q)}{ik_n - M_q' + \omega_Q - \epsilon''} (N_Q + f'') \\ & + \frac{N(M_q') + f(\epsilon'' + \omega_Q)}{ik_n + M_q' - \omega_Q - \epsilon''} \\ & \left. + \frac{1 + N(M_q') - f(\epsilon'' + \omega_Q)}{ik_n - M_q' - \omega_Q - \epsilon''} (1 + N_Q - f'') \right], \quad (6.27) \end{aligned}$$

where

$$M_q'^2 = (v_F q)^2 \left(1 - \frac{M_q}{\pi v_F}\right), \quad (6.28)$$

$$N(M'_q) = 1/(e^{\beta M'_q} - 1), \quad (6.29)$$

$$f(\epsilon'' \pm \omega) = 1/(e^{\beta(\epsilon'' \pm \omega)} + 1). \quad (6.30)$$

Now the imaginary part of the electron self-energy can be found by substituting $ik_n \rightarrow \epsilon + \delta$. From the above expression it follows that if we look at the high energy limit there will be a term which is proportional to T^2 . It is convenient to define

$$-Im\Sigma(\vec{k}) = (k_B T)\lambda(T), \quad (6.31)$$

$$\lambda(T) = (k_B T)4v_F \sum_{qQ} \frac{(\hat{\eta}_Q \cdot \vec{Q})^2}{\rho\omega_Q^2} \frac{q^2 M_q^2}{M_q'^2} \delta(\epsilon_k - \epsilon_{k+q+Q}). \quad (6.32)$$

The phonon energy and M'_q are neglected compared to the electron energy. Making use of the δ -function we obtain

$$\lambda(T) = (k_B T) \frac{16e^4 k_F^2}{\pi^4 \alpha v_F^2} \times I_2, \quad (6.33)$$

$$I_2 = \int_0^{\pi/2} dx \frac{x^2 \ln^2 x}{\sin^2 x (1 - \frac{2e^2}{\pi v_F} \ln x)}. \quad (6.34)$$

Numerical evaluation gives $I_2 \approx 0.68$. One obtains the same expression for λ for processes in the band and between bands since one takes $k \approx k_F$.

Besides the term proportional to T^2 there will be terms which have linear dependence on the temperature;

$$\lambda_1 = \frac{v_F}{8\pi^2} \int dq \int dQ \frac{(\hat{\eta}_Q \cdot \vec{Q})^2}{\rho\omega_Q^2} \frac{q^2 M_q^2}{M_q} \delta(\epsilon_k - \epsilon_{k+q+Q}), \quad (6.35)$$

$$\lambda_2 = \frac{\hbar v_F}{8\pi^2} \int dq \int dQ \frac{(\hat{\eta}_Q \cdot \vec{Q})^2}{\rho\omega_Q} \frac{q^2 M_q^2}{M_q^2} \delta(\epsilon_k - \epsilon_{k+q+Q}). \quad (6.36)$$

The term that has ω_Q in the denominator could be neglected because the mass of the ion is in the denominator too and as a whole this contribution can be neglected as small (as it was already pointed out). The term with ω_Q^2 can be evaluated and one is able to write the result

$$\lambda_1 = \frac{2e^4 k_F^3}{\pi^6 \alpha v_F} \times I_3, \quad (6.37)$$

$$I_3 = \int_0^{\pi/2} dx \frac{x^3 \ln^2 x}{\sin^2 x \sqrt{1 - \frac{2e^2}{\pi v_F} \ln x}}, \quad (6.38)$$

$$I_3 \approx 0.37. \quad (6.39)$$

The same calculation for graphene is more difficult technically. Analytical expression for P_q and ϵ_{RPA} cannot be derived [47], [48]. Thus, the above evaluation in 2D cannot be done in simple terms as it is demonstrated in 1D.

There are reported calculations in the literature that deal with the Coulomb interaction [45] in terms of bosonizations; calculations of the static polarizabilities of nanotubes are also available [59], but they do not treat the problem in the context of the electron-phonon interaction.

6.3 Exchange self-energy

6.3.1 Derivation of the exchange self-energy

One can look beyond the RPA approximation by assuming that the effects from the exchange phonon modulated electron-electron interaction is not small.

The exchange term is provided by writing the exchange pairing in the Green's function

$$\sum c_{\vec{k}+\vec{Q}+\vec{q}}^+ c_{\vec{k}'-\vec{q}}^+ c_{\vec{k}}^- c_{\vec{k}'}^- = - \sum c_{\vec{k}+\vec{Q}}^+ c_{\vec{k}}^- [f_{\vec{k}-\vec{q}} + f_{\vec{k}+\vec{q}+\vec{Q}}]. \quad (6.40)$$

The two terms arise from the different ways of pairing. In the problem for graphene the pairing has to be done for two different operators present in the expression - α and β . The exchange interaction up to a phase factor is written as

$$\begin{aligned} V_{exch} &= - \sum_{\vec{k}, \vec{q}, \vec{Q}} X_{\vec{Q}}(\vec{q} \cdot \vec{Q}) v_q \rho_e^2(q) [f_{\vec{k}+\vec{q}+\vec{Q}} + f_{\vec{k}-\vec{q}}] \\ &\times \left[\cos \frac{\theta(\vec{k} + \vec{Q}) - \theta(\vec{k})}{2} (\alpha_{\vec{k}+\vec{Q}}^+ \alpha_{\vec{k}}^- + \beta_{\vec{k}+\vec{Q}}^+ \beta_{\vec{k}}^-) \right. \\ &\left. + \sin \frac{\theta(\vec{k} + \vec{Q}) - \theta(\vec{k})}{2} (\alpha_{\vec{k}+\vec{Q}}^+ \beta_{\vec{k}}^- + \beta_{\vec{k}+\vec{Q}}^+ \alpha_{\vec{k}}^-) \right]. \quad (6.41) \end{aligned}$$

It is useful to express the Hamiltonian in the following way

$$V_{exch} = - \sum_{\vec{Q}} U(\vec{k}, \vec{Q}) X_{\vec{Q}} c_{\vec{k}+\vec{Q}}^{\dagger} c_{\vec{k}} A_{\vec{Q}}, \quad (6.42)$$

where we define

$$U(\vec{k}, \vec{Q})_{ii} = \hat{\eta}_{\vec{Q}} \cdot [(\vec{k} + \vec{Q})S(\vec{k} + \vec{Q}) - \vec{k}S(\vec{k})] \cos \frac{\theta(\vec{k} + \vec{Q}) - \theta(\vec{k})}{2}, \quad (6.43)$$

$$U(\vec{k}, \vec{Q})_{ie} = \hat{\eta}_{\vec{Q}} \cdot [(\vec{k} + \vec{Q})S(\vec{k} + \vec{Q}) - \vec{k}S(\vec{k})] \sin \frac{\theta(\vec{k} + \vec{Q}) - \theta(\vec{k})}{2}, \quad (6.44)$$

$$S(\vec{k}) = \frac{1}{k^2} \sum_{\vec{q}} M_{\vec{q}} f_{\vec{k}-\vec{q}} \vec{k} \cdot \vec{q}. \quad (6.45)$$

For small wave vectors \vec{Q} one is able to write

$$U(\vec{k}, \vec{Q}) \approx (\hat{\eta}_{\vec{Q}} \cdot \vec{Q}) S(\vec{k}). \quad (6.46)$$

Now the one-phonon self-energy is obtained

$$\Sigma(\vec{k}) = \frac{\hbar S^2(\vec{k})}{2\rho} \sum_{\vec{Q}} \frac{(\hat{\eta}_{\vec{Q}} \cdot \vec{Q})^2}{\omega_{\vec{Q}}} \left[\frac{N_{\vec{Q}} + f(\epsilon')}{ik_n - \epsilon' + \omega_{\vec{Q}}} + \frac{1 + N_{\vec{Q}} - f(\epsilon')}{ik_n - \epsilon' - \omega_{\vec{Q}}} \right], \quad (6.47)$$

$$f(\epsilon') = 1/(e^{\beta\epsilon'} + 1), \quad (6.48)$$

$$\epsilon' = \epsilon_{\vec{k}+\vec{Q}}. \quad (6.49)$$

There are four diagrams which correspond to eqn.(6.42). They are given in Fig.6.4. In the high temperature limit, neglecting the phonon energy compared to the electron energy,

$$-Im\Sigma(\vec{k}) = \pi(k_B T)\lambda, \quad (6.50)$$

$$\lambda = 2S^2(\vec{k}) \sum_{\vec{Q}} \frac{(\hat{\eta}_{\vec{Q}} \cdot \vec{Q})^2}{\rho\omega_{\vec{Q}}^2} \delta(\epsilon_{\vec{k}} - \epsilon_{\vec{k}+\vec{Q}}). \quad (6.51)$$

This is a general formula for the phonon-modulated exchange electron-electron interaction for these tight-binding systems. The imaginary part of the electron self-energy is proportional to T in the high temperature limit, as expected for

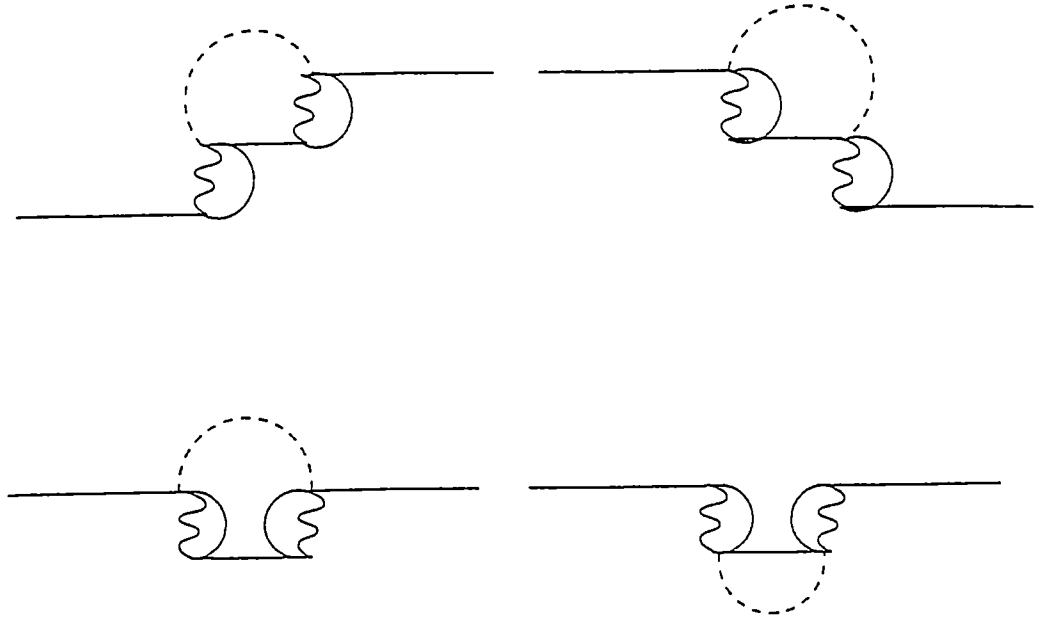


Figure 6.4: Diagrams for the exchange interaction with one phonon line

metals. Also it is evident that the matrix elements for this interaction display a deformation type - $M_Q = X_{\vec{Q}} S(\vec{k}_F) \vec{Q}$ - it is linear with Q with a “deformation constant” $S(\vec{k}_F)$.

6.3.2 Application to SWNT

The next step is to evaluate the function $S(\vec{k})$ which is contained in $U(\vec{k}, \vec{Q})$. In Appendix II the function $S(\vec{k})$ in 1D is derived.

In a more general way $S(x)$ could be written as

$$S_{1D}(x) = -\frac{e^2 k_F}{2\pi} J_{1D}(x). \quad (6.52)$$

In Fig.6.5 we present J_{1D} as a function of x . It is a smooth rising function, which takes its largest value at $x = 1$ where its value is taken. The expression from eqt.(6.51) is evaluated for longitudinal phonons. The energy dispersion for the nanotube is $\epsilon = J_0[1 - 2 \cos \frac{ka}{2}]$. The δ -function eliminates the integration over Q

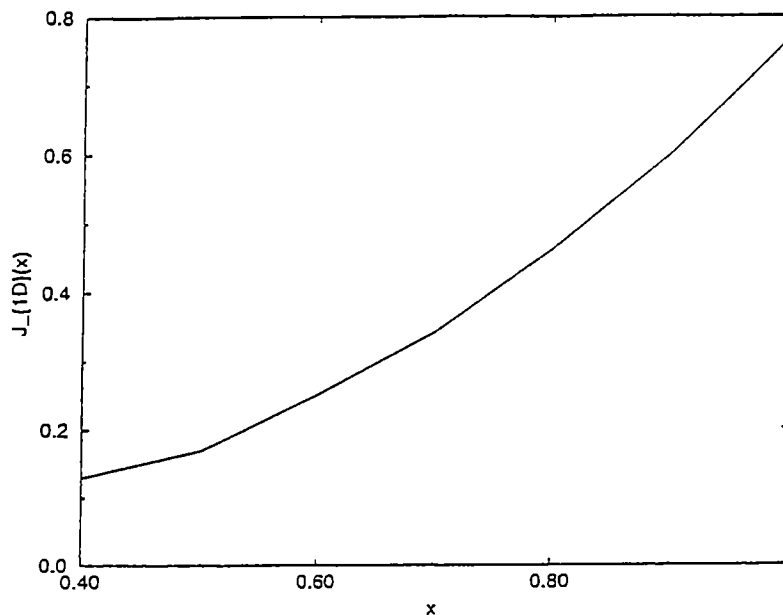


Figure 6.5: J as a function of x in 1D

$$\lambda = \frac{S_{1D}^2(x)k_F}{2\pi\alpha v_F}. \quad (6.53)$$

There is a direct analogy between the results for the ordinary electron-phonon interaction and the exchange interaction. The coupling constant λ is of the same form with different deformation constants.

6.3.3 Application to graphene

In 2D the same difficulties are encountered when the modulated hopping was considered. Eqn.(6.51) still holds, with the change that \vec{Q} and \vec{k} are two-dimensional. In Appendix III the evaluation of $S(\vec{k})$ in 2D is shown.

Again the S function can be written in the form

$$S_{2D}(x) = -\frac{e^2 k_F}{2\pi} J_{2D}(x), \quad (6.54)$$

where J_{2D} is discussed in Appendix III. Here we present it as a function of x on Fig.6.6. J_{2D} is maximum at $x = 1$, as the case with J_{1D} . For longitudinal phonons

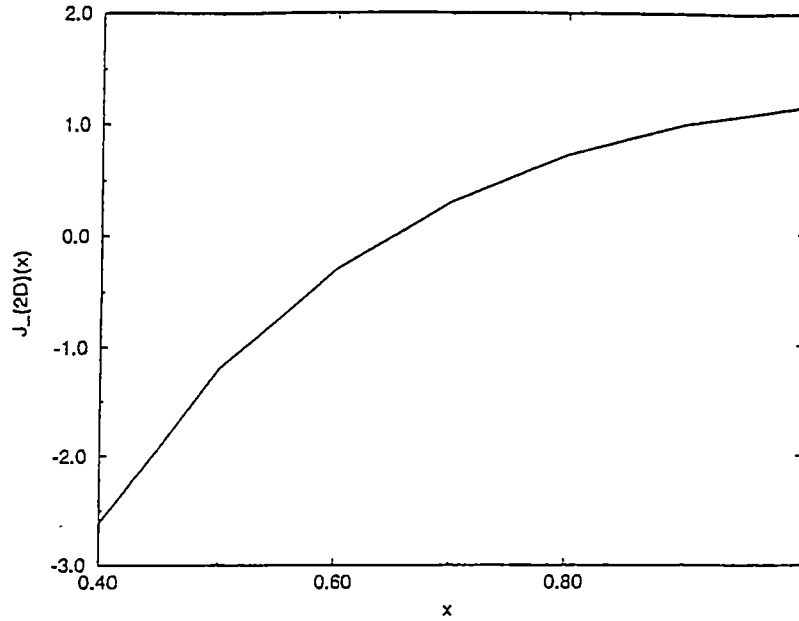


Figure 6.6: J as a function of x in 2D

only, the electron self-energy is

$$-Im\Sigma(k_F) = k_B T \frac{2S_{2D}^2(x)q_D}{\pi^4 \alpha v_F} \times I_1, \quad (6.55)$$

where I_1 was defined in eqn.(6.8).

It is not difficult to see that the results for the exchange electron self-energy could have been written by inspection using the expression for the electron-phonon interaction. The same integrals arise in both places. The only difference is in the contribution from the matrix elements. For the electron-phonon coupling the deformation constant D is present; for the phonon-modulated Coulomb interaction the function $S(x)$ plays the role of a deformation constant. Which contribution is large depends on whether D or $S(x)$ is larger.

In the next chapter we give numerical estimates for some transport properties for these low dimensional systems.

Chapter 7

Numerical Estimates of Some Transport Characteristics

7.1 Constant of interaction - λ

The results for the imaginary part of the electron self-energy due to different processes can be used to estimate some characteristics such as the electron lifetime and the electron-phonon coupling constant. They all depend on the imaginary part of the electron self-energy. We use the following relationship between τ - the lifetime and the imaginary part of the electron self-energy - $-Im\Sigma(\vec{k})$

$$\frac{\hbar}{2\tau} = -Im\Sigma(\vec{k}). \quad (7.1)$$

The previous chapter was devoted to find simple expressions for the contributions from different types of electron-phonon interaction. Here we intend to show that the numerical estimates for some of the transport properties for these low dimensional systems can contain contributions that have similar numerical values but different origin. It was shown that the $-Im\Sigma(\vec{k})$ is proportional to the temperature (at the high temperature limit) and it is also proportional to the coupling constant λ - eqn.(6.1). The coupling constant plays the deciding role which pro-

cess is dominating. All the physics is contained in it. According to the derivations from the previous chapter, for the modulated hopping

$$\lambda_{1D,hopp} = \frac{|D|^2 k_F}{2\pi\alpha v_F}, \quad (7.2)$$

$$\lambda_{2D,hopp} = \frac{2|D|^2 q_D}{\pi^4\alpha v_F}. \quad (7.3)$$

Using the result for the deformation constant from Ch.3, we obtain that $|D| = 11.72(1 - R) = 3.87 \text{ eV}$, and it is the same for graphene and for a tube. The constant v_F is found to be $v_F = 5.33 \text{ eV}\cdot\text{\AA}$. And finally, the constant α for graphite is taken as $\alpha = 8.98 \text{ N/m}^2$ - the number used to estimate R . The deformation constant is significantly reduced because of the factor $(1 - R)$. Therefore, we find that

$$\lambda_{1D,hopp} = 0.68, \quad (7.4)$$

$$\lambda_{2D,hopp} = 0.46. \quad (7.5)$$

Next the linear electron-phonon interaction is discussed. The only thing that changes is the deformation constant. Note that once the constant is found for one of the processes (in our case the modulated hopping) then for every other process we can use the following simple equation

$$\lambda_{e-p} = \frac{|\tilde{D}|^2 \times \lambda_{hopp}}{|D|^2}. \quad (7.6)$$

We find that $|\tilde{D}_{2D}| = 8\pi Z e^2 [\frac{3}{\alpha_2^2} - \frac{4}{\alpha_1^2}] = |\tilde{D}_{1D}|$. \tilde{D} depends on $\cos(\phi(\vec{k}, \vec{Q}))$ and $\sin(\phi(\vec{k}, \vec{Q}))$ (see Ch.3) which are taken to have their maximum value, so an upper limit for the coupling constant can be found. The values for α_i and α_e for carbon are listed in ref. [35]. Here we take a summation over them; the estimate for the deformation constant is $\tilde{D} \approx 0.89 \text{ eV}$. Therefore, the coupling constants for the tube and for graphene are found to be

$$\lambda_{1D,e-p} = 0.036, \quad (7.7)$$

$$\lambda_{2D,e-p} = 0.024. \quad (7.8)$$

Note that λ_{1D} and λ_{2D} are an order smaller than λ for the modulated hopping. Therefore, this makes the electron-phonon interaction due to the Coulomb potential to be unimportant compared to the modulated hopping.

When the RPA is discussed one notices that a linear term with T of the self-energy can be produced but since the ion mass is in the denominator, the general idea is that this contribution is not expected to be large. It turns out that analytical results can be derived for SWNT. A term which is proportional to T^2 of the self-energy can be produced, thus τ is proportional to T^2 . It is a signature of the ordinary electron-electron interaction. The lifetime can be made as big as one wants providing one goes at sufficiently low T . At room temperature this is a negligible factor compared to the dominant scattering mechanism. It is certainly necessary to go at very low temperatures (in order to avoid scattering by ionic vibrations) in very pure samples (in order to avoid impurity scattering) before one is able to see the characteristic T^2 -dependence. Define

$$\lambda(T)_{RPA} = (k_B T) \frac{16e^4 k_F^2}{\pi^4 \alpha v_F^2} \times I_2 \approx 0.002, \quad (7.9)$$

where the number is given at $T = 300 \text{ K}$. We conclude that the rate of this type of scattering proceeds is 10^2 slower than the modulated hopping and 10^1 slower than the linear electron-phonon interaction. But it is still much larger than the usual electron-electron contribution which for a typical metal is of the order of 10^4 slower than the one for the dominating electron-phonon scattering at room temperatures.

Also a linear term with the temperature was derived for the self-energy. This means that the lifetime is $\tau \sim T^{-1}$.

$$\lambda_{1D,RPA} = 0.035. \quad (7.10)$$

The value of τ shows that this process is an order slower than a typical relaxation time for metallic systems (involving only electron-phonon transitions). Thus, the

contribution from the RPA phonon modulated electron-electron interaction can be thrown away in agreement with the general derivation in Ch.6.

Now we consider the contribution from the phonon modulated Coulomb interaction from the exchange terms. Again $1/\tau \sim T$ - a characteristic feature for metallic systems. Thus, armchair SWNT and a layer of graphite are expected to display metallic behaviour according to this mechanism also. Here we show that the phonon modulated electron-electron interaction gives relatively large effects on the lifetime of the charge carriers. There is a complete analogy between the two expressions for the $Im\Sigma(k)$ concerning the ordinary electron-phonon and exchange phonon modulated electron-electron interactions. The only difference is in the coupling constants. In the second type of processes the deformation constant D is replaced by the function $S_{1D,2D}(x)$. We use eqn.(176) with a new deformation constant. Compare between $|D| = 3.87 \text{ eV}$ and $|S(x=1)_{1D}| = 3.02 \text{ eV}$ and $|S_{2D}(x=1)| = 4.56 \text{ eV}$. Therefore, one is able to estimate

$$\lambda_{1D,exch} = 0.41, \quad (7.11)$$

$$\lambda_{2D,exch} = 0.57. \quad (7.12)$$

The major conclusion that can be reached is that for these low dimensional tight binding systems the transport characteristics are expected to be dominated by two mechanisms - i) the first one is the traditional modulated hopping; ii) and the second one is the newly derived Coulomb interaction which arises due to the vibration modulated distance between the electrons. Both processes give similar contributions.

The above formulas and evaluations are done for perfect tubes and perfect sheets. All of the experimental measurements of SWNT are actually for ropes of SWNT. The transport processes are believed to be carried mainly along a single tube. The above expressions and estimates were done for one perfect armchair SWNT. But keeping in mind how they are synthesized one has to put defects

into the system also. This will change the answer somewhat especially at low temperatures [49].

7.2 Thermoelectric power of a perfect armchair SWNT

Now we look at another transport characteristic - the thermoelectric power (S). There are several reports in the literature about measuring S [50], [51]. Some of them concern ropes of armchair SWNT which are believed to contain mainly (10,10) tubes. S is measured to be positive and relatively big - $9 \mu V/K$ at room temperature. Calculations about S are also available, but they treat bundles or zigzag tubes [53], [52].

The model which is used to describe the tubes is a two-band model [56] with a linear dispersion of the energy with respect to the wave vector. For a perfect tube the concentration for the electrons and holes from the two bands is the same. We derived in the previous chapters that the relaxation times for transitions into the same band and between bands are the same also. The only difference is that the electric charge has opposite signs. Thus, using the model for a two-band system

$$S = \frac{\sigma_1 S_1 + \sigma_2 S_2}{\sigma_1 + \sigma_2}. \quad (7.13)$$

But $\sigma_1 = \sigma_2$ and the electric charge in S is contained to the first power according to

$$S = \frac{\pi^2}{3} \frac{k_B^2 T}{e} \left(\frac{\partial \ln \sigma}{\partial \epsilon} \right). \quad (7.14)$$

Therefore, the result for the thermopower is zero.

The same result is obtained if one considers the phonon drag contribution to S . Since the matrix elements for intraband and interband transitions are the same for the electron-phonon interaction, it follows from the two-band model that the result is zero again [57].

Therefore, the conclusion is that to obtain a nonzero answer for S one must include other effects in describing the tube. We keep in mind that in reality SWNT ropes are not perfect and other effects - such as scattering from magnetic impurities or topological defects might need to be introduced. The interaction of transition metal atoms with the carbon atoms is the subject of extensive research, both experimentally and theoretically [54], [55]. This interaction needs to be incorporated in the calculation of the thermopower. Also the junctions between tubes in a rope may change the electronic structure. As suggested by [58] a pseudogap is opened at the crossing point of the two lowest lying bands due to the intertube coupling.

Chapter 8

Discussion

Electron-phonon effects on two low-dimensional tight-binding systems are discussed in this work. A sheet of graphite represents a two dimensional solid and an armchair (10,10) single wall carbon nanotube represents a quasi-one dimensional solid. The initial intentions were to introduce and apply models for the description of a SWNT. Since these nanoparticles are formed by folding a sheet of graphite into a cylindrical form, it is useful to do that for graphene first and then apply them to a tube. It is instructive to see the similarities and differences between the two systems.

Carbon nanotubes are a newly discovered form of matter. All of their properties are affected by their geometrical structure and low dimensionality. Imagine a system made of carbon atoms only that can be made into a metal or a semiconductor just by changing the geometry - this is unique to solid state physics. These new systems offer the possibility to apply known models and to introduce new ones in order to understand better the physics of them.

First of all a new model is suggested for the description of the lattice dynamics of the systems. It has two parameters - α for the central force and β for the three body force that is responsible for the angle bending. The model is needed to

see exactly how the acoustic and optical modes depend on each other. With the presently available methods a simple analytical expression is not possible. If we make an appropriate choice for the numerical values for α and β we can reproduce all of the characteristic features of the phonon spectrum for graphene. For example we have chosen $\alpha = 8.98 \text{ N/m}^2$ and $\beta = 0.4 \text{ N/m}^2$. With this values a good description of the acoustic branches of the spectrum is achieved. Depending on which part of the graphene spectrum we are interested we can change the numbers for the parameters.

It is found that according to this model for small phonon wave vectors there is a relationship that connects the acoustic phonon modes to the optical phonon modes. This means that even though in the limit where only acoustic modes are important the optical ones cannot be neglected. This is a new result which is expected to affect some of the properties of these solids. Note that the formalism was developed for graphene first and the values for the parameters were found by fitting to the graphene spectrum. Then discrete boundary conditions were applied for the phonons of the (10,10) carbon nanotube - in this way one obtains a set of curves. For small \vec{Q} we retain only the one with $m = 0$ which the Γ point in the Brillouin zone.

One needs an appropriate model for the lattice vibrations in order to have a correct estimation of the electron-phonon coupling. We investigate three types of electron-phonon interaction - the modulated hopping, the linear electron-phonon interaction and the phonon modulated electron-electron interaction. The formalism is developed in a rather general way and it can be applied to other tight binding systems.

The potential of modulated hopping is assumed to be proportional to the distance between nearest neighbors only. This is true because the electrons are well localized around the atomic orbitals. Graphite has two atoms per unit cell and the conduction electrons are π -electrons. The interesting property of graphene

and a (10,10) tube is that only the two lowest lying energy bands are involved. These bands cross the Fermi level at the characteristic K -points of the Brillouin zone with a linear energy dispersion. Only transitions between these two bands are considered - the next available bands are at about $0.5 eV$.

The matrix elements for the modulated hopping are found for both systems. Again discrete boundary conditions are applied for the carbon nanotube. We find that the interaction is of deformation type and that the matrix elements depend not only on the acoustic modes, but on the optical ones also. With the help of the lattice vibration model we obtain that the deformation constant D for the interaction is reduced by a factor of $(1 - R)$ with $R = \frac{\alpha - \frac{9}{2}\beta}{\alpha + \frac{9}{2}\beta} \approx 0.67$. This is a new result that has not been obtained before.

The ordinary electron-phonon interaction is considered also. We find that again the coupling displays a deformation type and the deformation constant \tilde{D} depends on parameters that describe the electron and ion charge distributions.

The phonon modulated electron-electron interaction is a new type of interaction and it is present in every tight-binding system. It comes from the change of the distance between the electrons due to the ion vibrations in the solid. The matrix elements are calculated and they are a product of a part which depends on the phonon wave vector and a part that depends on the electron wave vector only.

The next thing which is done here is to estimate the electron-phonon coupling constant in terms of the many-body techniques, namely - construct the Feynman diagrams, write the formula for the electron self-energy and estimate the constant of the interaction. The diagram for the modulated hopping and for the linear electron-phonon interaction is the same and it is known. For the phonon modulated electron-electron interaction there are two contributions. One comes from the random phase approximation with one phonon line. The general expectation is that this effect is not large. We were able to obtain analytical expression for

Table 8.1: Numerical values for λ and τ for a tube

Process	coupling constant - λ	relaxation time - τ
modulated hopping	0.68	$1.9 * 10^{-14} s$
linear electron-phonon	0.036	$3.5 * 10^{-13} s$
RPA - T^2	0.002	$6.3 * 10^{-12} s$
RPA - linear	0.035	$3.6 * 10^{-13} s$
exchange	0.41	$3.07 * 10^{-14} s$

Table 8.2: Numerical values for λ and τ for graphene

Process	coupling constant - λ	relaxation time - τ
modulated hopping	0.46	$2.84 * 10^{-14} s$
linear electron-phonon	0.024	$5.3 * 10^{-13} s$
exchange	0.57	$2.2 * 10^{-14} s$

the carbon nanotube. It is shown that there is a term in the self-energy which is proportional to T^2 and it will be important at low temperatures and a term which is linear with T .

Another contribution comes from the exchange pairing of the electron operators. We have shown that this interaction can be written in such a way that again it displays a deformation type with a new deformation constant - $S(k_F)$. The constant is different for the two systems.

Some of the main results of the present work can be summarized into two tables. In Table 8.1 we present the calculated constant of interaction λ and the relaxation time τ for the armchair carbon nanotube. In Table 8.2 the same results are listed for graphene. Note that the formula for the coupling constant λ for all three types of electron-phonon interaction is the same. The only thing that

changes is the deformation constant. Therefore, the bigger the deformation constant, the bigger λ . Because $D_{1D,2D}$ and $S(k_F)_{1D,2D}$ are comparable the coupling constants are comparable also. The scattering times are presented in the tables, too. To obtain the total scattering time one uses the Matthiessen's rule. If there are several sources of scattering in the relaxation time approximation the rule implies that

$$\frac{1}{\tau} = \frac{1}{\tau_1} + \frac{1}{\tau_2} + \dots \quad (8.1)$$

Therefore, considering only the modulated hopping and the exchange interactions we obtain that $\tau_{1D} = 1.17 * 10^{-14}$ s and $\tau_{2D} = 1.24 * 10^{-14}$ s. Now one can compare with the relaxation time for Cu , for example - $\tau_{Cu} = 1.9 * 10^{-14}$ s. Thus, the conclusion is that the relaxation time for graphene and the armchair single wall carbon nanotube is roughly 1/2 of τ_{Cu} . From here it is easy to give some estimates about the electrical conductivity of the two systems. We use the standart formula [8], [59]

$$\sigma = \frac{ne^2\tau}{m} \quad (8.2)$$

with the appropriate value for the relaxation time τ . For 2D graphite n is taken to be approximately 10^{23} cm^{-3} according to [34]. Therefore, $\sigma_{graph} \approx 3.5 * 10^5 \frac{1}{\Omega.cm}$. This value is of the order of the value for the conductivity for copper. Notice that the present model does not apply to pure 3D graphite. The reason is that the Fermi surface in 3D is largely modified by the coupling between layers. This implies that the phonons perpendicular to the surface of graphene are also important. Therefore, one considers the region where the band structure is essentially two-dimensional and the present model can be applied.

For the carbon nanotube we perform similar estimates. One takes the electron concentration $n \approx 10^{21}$ cm^{-3} [16]. Thus, one obtains that $\sigma_{tube} \approx 3.29 * 10^3 \frac{1}{\Omega.cm}$. This is in the range of the observed conductivities of ropes formed from single wall carbon nanotubes. The observed resistivities are in the range of 0.01-0.001

$\Omega.cm$ [60], [61]. The transport in the ropes is carried mainly by the individual tubes. It is evident that the measured and estimated conductivity, although indicative of the metallic character, are far below that of copper.

Finally, the last remark we would like to make is that all of the above considerations and estimations are done for graphene and a single wall carbon nanotube free of defects.

Bibliography

Bibliography

- [1] P. Butcher, N.H. March, and M.P. Tosi, *Physics of Low-Dimensional Semiconductor Structures* (Plenum Press, New York, 1993)
- [2] S. Iijima and T. Ichihashi, *Nature* **363**, (1993)
- [3] J.W. Mintmire, B.I. Dunlap and C.T. White, *Phys.Rev.Lett.* **68**, 631 (1992)
- [4] G.D. Mahan and L.M. Woods, submitted for publication
- [5] K.C. Haas, *Phys.Rev. B* **46**, 139 (1992)
- [6] A.A. Ahmedieh and H.A. Rafizadeh, *Phys.Rev. B* **7**, 4527 (1973)
- [7] R.A. Jishi, L. Venkataraman, M.S. Dresselhaus, and G. Dresselhaus, *Phys.Rev. B* **51**, 11176 (1995)
- [8] N.W. Ashcroft and N.D. Mermin, *Solid State Physics* (Saunders College Publications, Orlando, 1976)
- [9] T.W. Ebessen et al., *Chem.Phys.Lett.* **209**, 83 (1993)
- [10] K. Sattler, *Carbon* **33**, 915 (1995)
- [11] T. Gue et al., *Chem.Phys.Lett.* **243**, 49 (1995)
- [12] Y.H. Lee, S.G. Kim, and D. Tomanek, *Phys.Rev.Lett.* **78**, 2393 (1997)

- [13] L. Chiko et al., Phys.Rev.Lett. **76**, 971 (1996)
- [14] J. Tersoff and R.S.Ruoff, Phys.Rev.Lett. **73**, 676 (1994)
- [15] S.I. Dunlap, Phys.Rev. B **49**, 5643 (1994)
- [16] R.A. Jishi, M.S. Dresselhaus, and G. Dresselhaus, Phys.Rev. B **47**, 16671 (1993)
- [17] D.S. Bethune et. al., Nature **363**, 603 (1993)
- [18] C. Journet et. al., Nature **388**, 388 (1997)
- [19] A.W. Overhauser, Physics **1**, 307 (1965)
- [20] R.A. Jishi, L.Venkataraman, M.S. Dresselhaus, and G. Dresselhaus, Chem.Phys.Lett. **209**, 77 (1993)
- [21] P.C. Eklund, J.M. Holden, and R.A. Jishi, Carbon **33**, 959 (1995)
- [22] R.A. Jishi, D. Inomata, K. Nakao, M.S. Dresselhaus, and G. Dresselhaus, J.Phys.Soc.Japan **63**, 2252 (1994)
- [23] H. Hiura, T.W. Ebessen, K. Tanigaki, and H. Takahashi, Chem.Phys. Lett. **202**, 509 (1993)
- [24] A. Charlier et al., Phys.Rev. B **57**, 6689 (1998)
- [25] F.H. Stillinger and T.A. Weber, Phys.Rev B **31**, 5262 (1985)
- [26] R.A. Jishi, L. Venkataraman, M.S. Dresselhaus, and G. Dresselhaus, Phys.Rev. B **47**, 16671 (1993)
- [27] J. Callaway, *Quantum Theory of the Solid State*(Academic Press, Inc., San Diego, 1991)
- [28] P.R. Wallace, Phys.Rev. **71**, 622 (1947)

- [29] S. Barisic, J. Labbe, and J. Friedel, *Phys.Rev.Lett.* **25**, 919 (1970)
- [30] G.D. Mahan, *Many-Particle Physics* (Plenum Press, New York, 1990)
- [31] J.M. Ziman, *Electrons and Phonons* (The University Press, Oxford, 1967)
- [32] M.F. Bishop and A.W. Overhauser, *Phys.Rev. B* **23**, 3627 (1981)
- [33] A.H. Macdonald, R. Taylor and D.W.J. Geldhardt, *Phys.Rev. B* **23**, 2718 (1981)
- [34] L. Pietronero, S. Strassler and H.Z. Zeller, *Phys.Rev. B* **22**, 904 (1980)
- [35] E. Clementi and C. Roetti, *Atomic Data and Nuclear Data Tables* **14**, 282 (1974)
- [36] S. Iijima, *Nature* **354**, 56 (1991)
- [37] A. Thess et. al., *Science* **273**, 483 (1996)
- [38] R. Saito et. al., *Phys.Rev. B* **46**, 1804 (1992)
- [39] M.S. Dresselhaus, G. Dresselhaus and P.C. Eklund, *Science of Fullerenes and Carbon Nanotubes* (Academic Press, San Diego, 1996)
- [40] R.A. Jishi, M.S. Dresselhaus and G. Dresselhaus, *Phys.Rev. B* **48**, 11385 (1993)
- [41] M.F. Lin and K.W.-K. Shung, *Phys.Rev. B* **47**, 6617 (1993)
- [42] Ch. Kittel, *Introduction to Solid State Physics* (John Wiley, Inc., New York, 1996)
- [43] K. Gross, *Many-Particle Physics* (Academic Press, New York, 1997)
- [44] M.F. Lin, D.S. Chuu and K.W.-K. Shung, *Phys.Rev. B* **56**, 1430 (1997)

- [45] R. Egger and A.O.Gogolin, Phys.Rev.Lett. **79**, 5082 (1997)
- [46] L.X. Lorin, S.G. Louie and M.L. Cohen, Phys.Rev. B **52**, 8541 (1995)
- [47] J. Blinkowski et al., J.Phys. (Paris) **41**, 667 (1980)
- [48] K. W.-K. Shung, Phys.Rev. B **34**, 979 (1986)
- [49] M. Antram, and T. Govindan, Phys.Rev. B **58**, 4882 (1998)
- [50] J. Hone et al., Phys.Rev.Lett. **80**, 1042 (1998)
- [51] L. Grigorian et al., Phys.Rev. B **58**, R4198 (1998)
- [52] M.F. Lin, D.S. Chuu and K.W.-K. Shung, Phys.Rev. B **53**, 11186 (1996)
- [53] M. Tian et.al., J.Appl.Phys. **82**, 3164 (1997)
- [54] M. Baumer, J. Libuda and H-J. Freund, Surf.Sci. **327**, 321 (1995)
- [55] L. Chen, R. Wu, N. Kioussis and J.R. Blanco, J.Appl.Phys. **81**, 4161 (1997)
- [56] F.J. Blatt, P.A. Schroeder, C.L. Foiles and D. Craig, *Thermoelectric Power of Metals* (Plenum Press, New York, 1976)
- [57] M. Bailin, Phys.Rev. **157**, 480 (1967)
- [58] Y.-K. Kwon, S. Saito, and D. Tomanek, Phys.Rev. B **58**, R13314 (1998)
- [59] L.X. Benedict et al., Phys. Rev B **52**, 14935 (1995)
- [60] T.W. Ebessen and P.M. Ajayan, Nature (London) **358**, 220 (1992)
- [61] L. Langer et al., J.Mat.Res. **9**, 927 (1994)

Appendices

Appendix A

Calculation of the Polarization Factor For the SWNT

Here we derive the general expression for the polarization factor in 1D. Start with the definition

$$P_q = \frac{1}{\pi} \int_{-k_F}^{k_F} dk \frac{f_k - f_{k+q}}{iq_n + \epsilon_k - \epsilon_{k+q}} \quad (\text{A.1})$$

There are two contributions - from the interband transitions (P_{q1}) and from the intraband transitions (P_{q2}). P_{q1} can be found analytically using that the energy dispersion is linear with the wave vector

$$P_{q1} = \frac{2}{\pi} \int dk (f_k - f_{k+q}) \frac{v_F q}{(v_F q)^2 - (iq_n)^2} \quad (\text{A.2})$$

$$P_{q1} = \frac{2}{\pi \beta v_F} \ln \frac{e^{\beta v_F q/2} \cosh \frac{\beta v_F q}{2} \cosh \beta v_F k_F}{\cosh \beta v_F (k_F - q/2)} \frac{v_F q}{(v_F q)^2 - (iq_n)^2} \quad (\text{A.3})$$

$$P_{q1} \approx \frac{v_F q^2}{\pi (v_F q)^2 - (iq_n)^2} \quad (\text{A.4})$$

The limit $q \rightarrow 0$ is taken in eqn.(A.3).

The other contribution to P_q is given by

$$P_{q2} = \frac{2}{\pi} \int dk \frac{2v_F k_F + 2v_F k - v_F q}{(2v_F(k_F + k - q/2))^2 - (iq_n)^2} \quad (\text{A.5})$$

$$P_{q_2} = \frac{2}{\pi v_F} \ln \frac{(4v_F k_F + v_F q)^2 - (iq_n)^2}{(v_F q)^2 - (iq_n)^2} \quad (\text{A.6})$$

In obtaining the last expression we have used that the Fermi distribution function at zero temperature is a step function and it restricts the integration to the first Brillouin zone.

Appendix B

Calculation of $S(k)$ for a tube

The function $S(k)$ in 1D is evaluated here. Using the definition we have

$$S(k) = \frac{1}{2\pi k} \int dq M_q f_{k-q} \quad (\text{B.1})$$

Now the change of variables $k - q \rightarrow k$ is made and the integration is restricted in the first Brillouin zone. Thus,

$$M_q = 2e^2 \ln \frac{q}{k_F} \quad (\text{B.2})$$

$$S(k) = -\frac{e^2 k_F}{2\pi x} [(1+x)^2 \ln|1+x| - (1-x)^2 \ln|1-x| - 2x] \quad (\text{B.3})$$

$$S(k) = -\frac{e^2 k_F}{2\pi} J_{1D}(x) \quad (\text{B.4})$$

where $x = k/k_F$. Since we are interested at processes around the Fermi level we take $x = 1$ and the above expressions become

$$S(1) = -\frac{e^2 k_F}{2\pi} J_{1D}(1) \quad (\text{B.5})$$

$$J_{1D}(1) = 4 \ln 2 - 2 \quad (\text{B.6})$$

Therefore, $J_{1D}(x) \approx 0.77$.

Appendix C

Calculation of $S(\vec{k})$ for Graphene

The analytical evaluation of $S(\vec{k})$ in 2D is more difficult because the integration now becomes two-dimensional. After the appropriate change of variables $\vec{k}-\vec{q} \rightarrow \vec{k}$ we obtain

$$S(k)_{2D} = -\frac{e^2}{2\pi k} \int_0^{k_F} dk' \int_0^{2\pi} d\phi \frac{kk' - k'^2 \cos \phi}{\sqrt{k'^2 + k^2 - 2kk' \cos \phi}} \quad (C.1)$$

If the integration over ϕ is done first, this leads to elliptical integrals. It turns out that simple results can be obtained if we integrate over k' first. With $x = k/k_F$ the above expression becomes

$$\begin{aligned} S_{2D}(x) &= -\frac{e^2 k_F}{2\pi x} \int_0^{2\pi} d\phi \left[\left(\frac{3}{2} x \cos \phi - x^2 \right) \right. \\ &+ \left(x - \frac{1 + 3x \cos \phi}{2} \right) \sqrt{1 + x^2 - 2x \cos \phi} \\ &+ \left. x^2 \left(\cos \phi - \frac{3 \cos^2 \phi - 1}{2} \right) \ln \frac{\sqrt{1 + x^2 - 2x \cos \phi} + 1 - x \cos \phi}{x(1 - \cos \phi)} \right] \end{aligned} \quad (C.2)$$

Now at $x = 1$ the $S(x)$ -function can be written in the usual form -

$$S(x) = -\frac{e^2 k_F}{2\pi} J_{2D}(x) \quad (C.3)$$

$J_{2D}(x)$ is evaluated when $x = 1$.

$$J_{2D}(x = 1) = \int_0^{2\pi} d\phi \left[\left(\frac{3}{2} \cos \phi - 1 \right) + (1 - 3 \cos \phi) \sin \frac{\phi}{2} \right]$$

$$+ \frac{1}{2}(2 \cos \phi - 3 \cos^2 \phi + 1) \ln\left(1 + \frac{1}{\sin \frac{\phi}{2}}\right)] \quad (\text{C.4})$$

The above integral can be done and we obtain that $J_{2D}(x=1) \approx 1.17$.

Vita

Lilia Woods was born on May 28, 1969 in Kyustendil - a small town near the capital of Bulgaria, Sofia. She graduated with honors from a high school specialized in economy in May, 1988. She entered the Physics Department of Sofia University (SUPD) in Sofia in August, 1988. After 5-year course of study, she graduated from SUPD with honors in August, 1993 and received a Master of Science Degree in Nuclear Physics.

After working for a year as a high school teacher, in August, 1994 she entered the Ph.D. program in Physics at the University of Tennessee, Knoxville. From August, 1994 until July, 1996 she worked as a Graduate Teaching Assistant at the Physics Department. In September, 1996 she started working for Prof. Gerald D. Mahan as a Graduate Research Assistant.

Lilia Woods is a permanent US Resident. She is a coauthor of three articles and a patent.

1. G.D. Mahan and L.M. Woods, "Phonon Modulated Electron- Electron Interactions", Phys.Rev B, submitted for publication.
2. G.D. Mahan and L.M. Woods, "Multilayer Thermionic Refrigeration", Phys.Rev.Lett. **80**, 4016 (1998)
3. L.M. Woods and G.D. Mahan, "Nonlinear Electron-Phonon Heat Exchange", Phys.Rev. B **57**, 7679 (1998)
4. US Patent Provisional Application - U.S. Serial No. 09/148,015, "Method and Apparatus for Multilayer Thermionic Thermal Transport"